VISION-BASED MONITORING AND CONTROL OF FIBER LASER WELDING

A Thesis Submitted to the
Graduate School of Engineering and Sciences of
İzmir Institute of Technology
in Partial Fulfillment of the Requirements for the Degree of

MASTER OF SCIENCE

in Mechanical Engineering

By
Emre TAVKAYA

July 2014
İZMİR

We approve the thesis of **Emre TAVKAYA**

Examining Committee Members:

Prof. Dr. Serhan ÖZDEMİR
Department of Mechanical Engineering, Izmir Institute of Technology

Assoc. Prof. Dr. Enver TATLICIOĞLU
Department of Electrical & Electronics Engineering, Izmir Institute of Technology

Assist. Prof. Dr. Mehmet İsmet Can DEDE
Department of Mechanical Engineering, Izmir Institute of Technology

Assist. Prof. Dr. Onursal ÖNEN
Department of Mechanical Engineering, İzmir Institute of Technology

Gökay PÜSKÜLCÜ, M.Sc.
Mechanical Engineer, Lazertek Tasarım

14 July 2014

Assist. Prof. Dr. Mehmet İsmet Can DEDE
Supervisor, Department of Mechanical Engineering, İzmir Institute of Technology

Prof.Dr. Metin TANOĞLU
Head of the Department of
Mechanical Engineering

Prof.Dr. R.Tuğrul SENGER
Dean of the Graduate School of
Engineering and Sciences

ACKNOWLEDGMENTS

First of all, I would like to express my gratitude to my supervisor Assist. Prof. Dr. Mehmet İsmet Can Dede for his invaluable supervision, guidance and care throughout this thesis.

I would like to thank the jury members; Prof. Dr. Serhan Özdemir, Assoc. Prof. Dr. Enver Tatlıcıoğlu, Assist. Prof. Dr. Onursal Önen and M.Sc. Gökay Püskülcü for their attendance at my thesis defence seminar and valuable recommendations.

I am also grateful to Gökay Püskülcü and Fikret Koçlular, Co-founders and Production Managers of Lazertek Company, for their permission and sharing their knowledge during site survey and experimental stage of this study.

I would like to thank to Hakan Hisli, Sales Specialist at Kibele-PIMS Company, for his encouragement and support during site survey on machine vision and vision system components.

I am also grateful to Emre Uzunoğlu and other Iztech Robotics Laboratory Staff for their valuable suggestions and friendship.

My special thanks to my dear friends Oğuzhan Zilci, Sencer Kan and Yusuf Alagöz for their endless support, patient and friendship. Furthermore, my special thanks to my special friend Çisel Boztepe for her endless patient encouragement and support during this study.

Finally, I am indebted to my father Selahattin Tavkaya, my mother Adile Tavkaya, my sister Elif Tavkaya and my brother Özgür Öztop for their endless love and patient throughout my life. This thesis is dedicated to them.

ABSTRACT

VISION-BASED MONITORING AND CONTROL OF FIBER LASER WELDING

Laser welding is an advanced emission process that applies the converted laser beam energy to join pieces by melting and welding them together. Fiber lasers, with their high efficiency, continuous wave and shorter wavelength, are mostly useful for deep penetration welding of materials. To avoid the defects in an automated fiber laser welding process such as pores, cracks or blow-out holes and to make the welding process controllable, off-line pre-process is required. Tuning welding parameters is critical during this stage since modeling of the process is hard and parameters change with respect to material and thickness. Therefore, real-time control of the laser welding becomes a challenge due to uncertainties in the process. A solution to such problem could be a vision-based monitoring and control system, which uses a path modification algorithm that matches CAD-based (Computer Aided Design-based) path data to target path before welding. In this thesis, a vision-based path modification algorithm is developed to determine the orientation of target welding path. Two subsystems are used in this developed technique including; a machine vision system and a CNC system. These subsystems are integrated through developed vision algorithm and subroutine logic of CNC system by calculating laser spot position on workpiece during operation. As a result of implemented technique, welding path modification data is stored as a CNC subprogram (file) under the CNC main program so that operational modification is made without the need of any change on the main CNC program.

The proposed method is experimentally tested to assess the performance of the monitoring and control technique on line and curve welding paths for mild steel and stainless steel materials with two different material thicknesses. The accuracy of the measurements is carried out by comparing the measured and computed offset values that are exported from the vision algorithm with reference to effective laser beam diameter. The results of tests indicate that the vision system accuracy varies between %85 and %95 for 600 micron effective laser beam size. For thinner materials less than 1 millimeter, due to smaller effective laser beam size requirements, system performance is found to be decreased down to %58-70 as a result of 400 micron effective laser beam size.

ÖZET

FİBER LAZER KAYNAĞININ GÖRÜNTÜ TABANLI GÖZLEMLENMESİ VE DENETİMİ

Lazer kaynağı, kaynak ile birleştirilecek parçaların, dönüştürülen lazer ışın enerjisini yüksek verimde odaklayarak ısıtılarak eritilmesi ve birleştirilmesi işlemidir. Derin penetrasyon gerektiren uygulamalarda lazer kaynağı, yüksek verimliliği, düşük dalga boyu ve sürekliliği gibi önemli özelliklerinden dolayı tercih edilir. Kırılma, çatlama ve yırtılma gibi olası kaynak hatalarını önlemek ve kaynak işlemini kontrol edebilmek için gerçek zamanlı olmayan ön işlem uygulaması gerekmektedir. İşlemin modellenmesi zor olduğundan ve parametrelerin malzemeye ve kalınlığa göre değiştiğinden ötürü bu aşamada kaynak parametrelerinin ayarlanması kritiktir. Bu belirsizlikten ötürü gerçek zamanlı lazer kaynak proses için zor bir uygulamadır. Böylesi bir probleme çözüm olarak, kaynak öncesinde, kaynak çizgisi ile BDT (Bilgisayar Destekli Tasarım) ortamında hazırlanmış bir çizginin birbiriyle eşleşmesi amacıyla, görüntü temelli izleme ve kontrol sistemi geliştirilebilir. Bu tezin kapsamında, görüntü temelli kaynak çizgisi düzeltme algoritması geliştirilerek kaynak yapılacak çizginin pozisyonu belirlenmiştir. Uygulanan teknikte, CNC sistemi ve makine görüntüleme sistemi olarak iki ana sistem kullanılmıştır. Bu sistemlerin entegrasyonu için, görüntü işleme algoritması ve CNC ana döngü mantığı kullanılarak işlem sırasında lazer ışınının kaynağı yapılacak parça üzerindeki pozisyonu hesaplanmıştır. Tekniğin uygulanması sonucunda hesaplanan düzeltmeler, CNC programının bulunduğu dosya altına depolanarak mevcut CNC programı üzerinde herhangi bir değişikliğe gerek kalmadan uygulanmıştır.

İzleme ve kontrol tekniğinin performansı düz ve eğri kaynak çizgileri için farklı iki kalınlıktaki soğuk haddelenmiş çelik ve paslanmaz çelik malzemeleri üzerinde yapılan deneysel testler sonucunda belirlenmiştir. Ölçümlerin kesinliği, ölçülen ve görüntü algoritmasından elde edilen değerlerin efektif lazer ışını çapı referans alınarak karşılaştırılması sonucu belirlenmiştir. Test sonuçlarına gore, 600 mikron efektif lazer ışını çapı için sistem performansı %85 ile %95 aralığında bulunmuştur. 1 milimetreden daha ince malzemelerde oluşan daha küçük efektif lazer ışını çapı gereksinimleri sonucunda, 400 mikron efektif lazer ışını çapı için sistem performansı yeniden ölçülerek %58 ile %70 aralığında bulunmuştur.

TABLE OF CONTENTS

LIST OF FIGURES

Figure **Page**

LIST OF TABLES

CHAPTER 1

INTRODUCTION

Laser welding is one of the most innovative manufacturing processes in industry of 21th century. Compared to other conventional welding techniques, laser welding is remarkably good at guiding and focusing the energy source on the workpiece. With the advantage of producing high energy densities at the weld zone (Figure 1.1), laser welding is preferred at high speed welding applications in automotive, electronics and home appliance industries. It is inevitable that laser welding will find greater place in production field in the future.

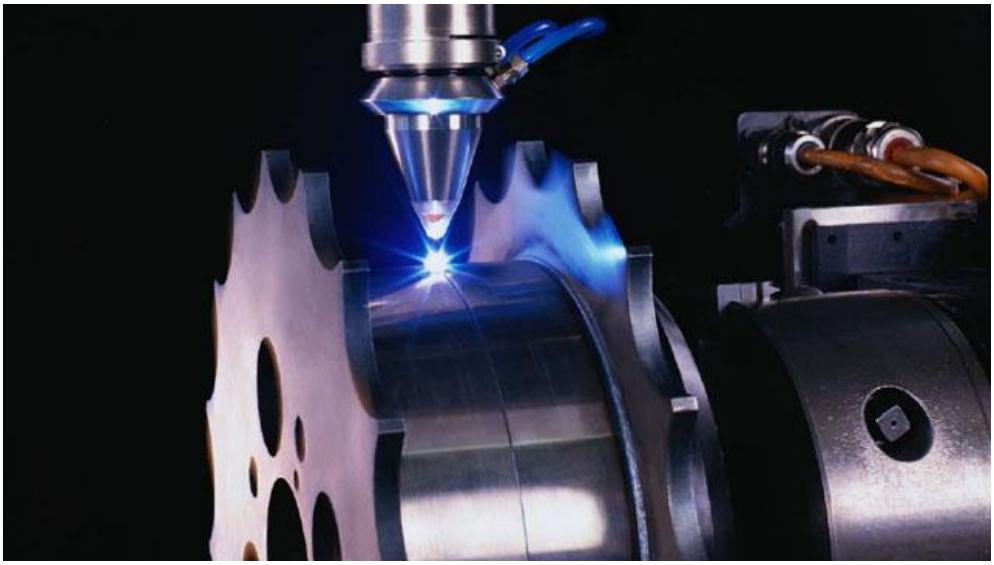

Figure 1.1. Trumpf-laser welding.
(Source: Trumpf-laser)

Welding is an extensively used method in metal industry. Complex shaped parts can be produced by using a welding system with simple materials such as plate or block. The basis of welding is applying high energy to a joint of the two materials to be merged, or in combination with a filling material to ensure the adhesion of the melting materials by localized heat. The high energy is provided by an outer power supply (Dahotre and Harimkar 2008, Timings 2008).

One of the outer power supplies for welding is laser beam. The biggest difference of laser beam from other energy sources is its ability to focus the energy to a desired point where the workpieces are merged. Laser welding is based on this concentrated energy, which is from the laser beam generator through various optical materials focused on the composition area to melt two materials as a result of overheating. Additional materials can be added in some applications during welding with a laser beam, or a laser beam can be used together with other conventional welding methods (Jokinen 2004).

Laser beam and its stimulating power have to be defined properly. The focused laser beam has one of the highest power densities, like an electron beam. Laser welding is a process of routing that laser beam's high-energy. A comparison is illustrated in Figure 1.2 that defines the fusion zone profile of different types of welding processes.

Process	Heat source intensity ($W\ m^{-2}$)	Fusion zone profile
Flux-shielded arc welding	5×10^6–10^8	
Gas-shielded arc welding	5×10^6–10^8	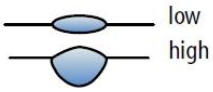
Plasma	5×10^6–10^{10}	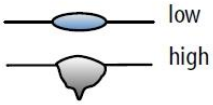
Laser or electron beam	10^{10}–10^{12}	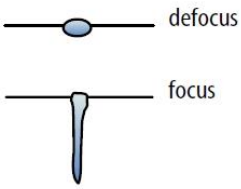

Figure 1.2. Relative power densities of different welding processes.
(Source: Steen and Mazumder 2010)

All materials will evaporate if the energy can be absorbed at high power densities. The result of this absorption is known as welding. During this absorption, as the keyhole geometry (molten pool) gets deeper, joining efficiency (penetration) is increased. Lasers offer a wide range of welding capabilities such as spot, conduction, penetration or hybrid since their power density absorption efficiency is higher than

conventional welding processes. Nevertheless, good beam quality is preferred in laser technology for better efficiency (Steen and Mazumder 2010).

Laser welding relies on a finely focused beam to achieve intended penetration. Focusing process is important for the material to absorb the energy. Thus, laser beam, which is provided by the laser source, is collected and focused by an optical lens on workpiece (shown in Figure 1.3 as "Focusing Lens"). Shielding gas (Argon, Helium and Nitrogen) is used to shroud the heated zone for steady welding and to prevent rapid oxidation due to atmospheric oxygen, which is shown in Figure 1.3 as inserted from the "Shielding gas inlet". Mechanical properties are unaffected by cover gas and also weld takes brighter appearance that ensures a better result cosmetically. Today, compact laser welding heads are produced by companies with compatibility for different welding applications (Precitec, Lasermech).

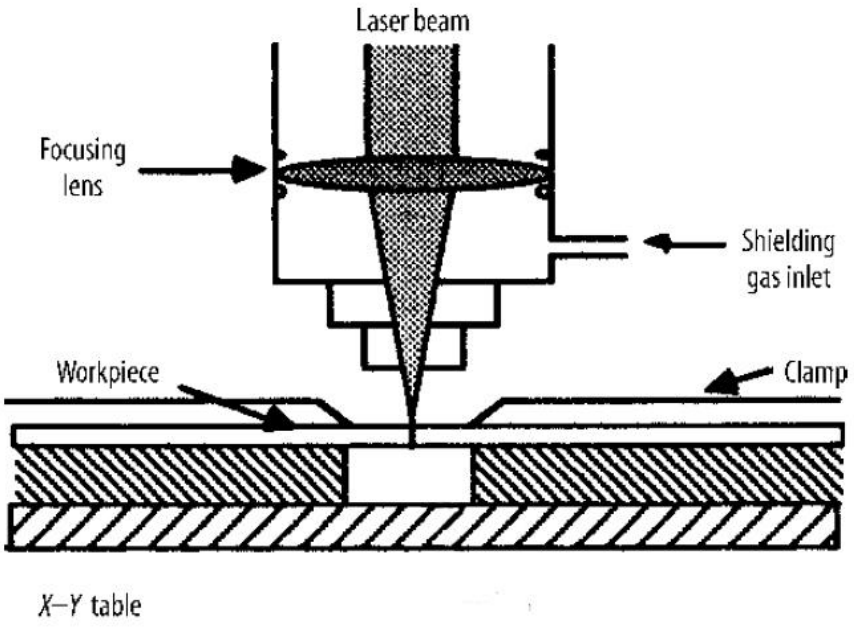

Figure 1.3. General arrangement of laser welding.
(Source: Steen and Mazumder 2010)

1.1. Applications

Materials with different melting points can be joined by using a laser welding method. Due to the small amount of molten material and short-controllable melting period, the materials that cannot be combined with conventional welding methods can be welded together. Filler material can be used if necessary. Laser welding applications have a wide range of use in industry. Laser welding usage in various applications depend on required laser beam wavelength, wave type (continuous or pulsed etc.), heat affected zone sensitivity, material type, penetration depth and welding type.

Advantages of laser welding with respect to the conventional welding methods are that laser welding has low distortion, high speed and a smaller size of heat affected zone. There are prominent features of laser welding such as applying a beam of light that is monochromatic, collimated and sufficient power density. By adjusting power density, very high values of irradiance and necessary localized heating can be easily achieved. Because the light is collimated and monochromatic, the heat-affected zone can be very small without the need of post-processing. This capability is required in case of spot welding with an extremely small weld diameter. System set-up, integration and configuration are also relatively easier and there is no contact of any material with the workpiece during operation.

The disadvantage of laser welding is its initial cost and limited capability in terms of having depth of penetration to be related directly to laser system power. Careful process monitoring, control and parameter scheduling are also required to avoid material vaporization due to high temperature around the weld (Na et al. 2010).

When all these advantages and disadvantages are considered, laser welding found itself applications in various industries such as construction, mold and dye, automotive, marine, electronics, medical, plastic processing, heating, home appliances, textile and metal processing. A few examples are described as follows:

In electronics:

1. Hermetically sealing electronic capsules, which is possible owing to the low heat affected zone.

In metal processing:

2. Welding of endless welded tubes is possible with the single joining spots or continuous wave mode (Figure 1.4). In pulsed mode, the short laser pulses are generated by the laser pump. Power, duration and frequency of the laser pulses are important parameters for material processing (Trumpf-laser 2014).

Figure 1.4. Endless laser welded tubes.
(Source: Trumpf-laser)

3. Welding of complex shapes prior to pressing (Matsunawa 1991, Billion and Fabre 1991).

4. Welding layered shaving blades (Steen and Mazumder 2010).

5. Multiple welds in TV tubes – This application uses 15 fibres placed at different locations in an assembly jig to make 15 spot welds sequentially from one Nd:YAG laser. The commercial advantage is the time saved in locating the spot welder (Brander et al. 2000).

6. Sheet metal products such as washing machines and heat exchangers – One technique being used on some heat exchangers and aircraft parts is to weld a flat pack of two or more layers in an appropriate pattern and then blow the shape up with compressed gas or hydraulically (Steen and Mazumder 2010).

In automotive:

7. Welding of transmission systems for cars – Taking advantage of the low distortion and the possibility of focusing near to potentially magnetic material.

8. Laser welding methods are being used more and more for three-dimensional welding of car and aircraft components – This is a new application area since most other welding processes cannot be controlled well enough for three-dimensional manipulation and monitoring. A demonstration for laser welding used on a car is illustrated in Figure 1.5.

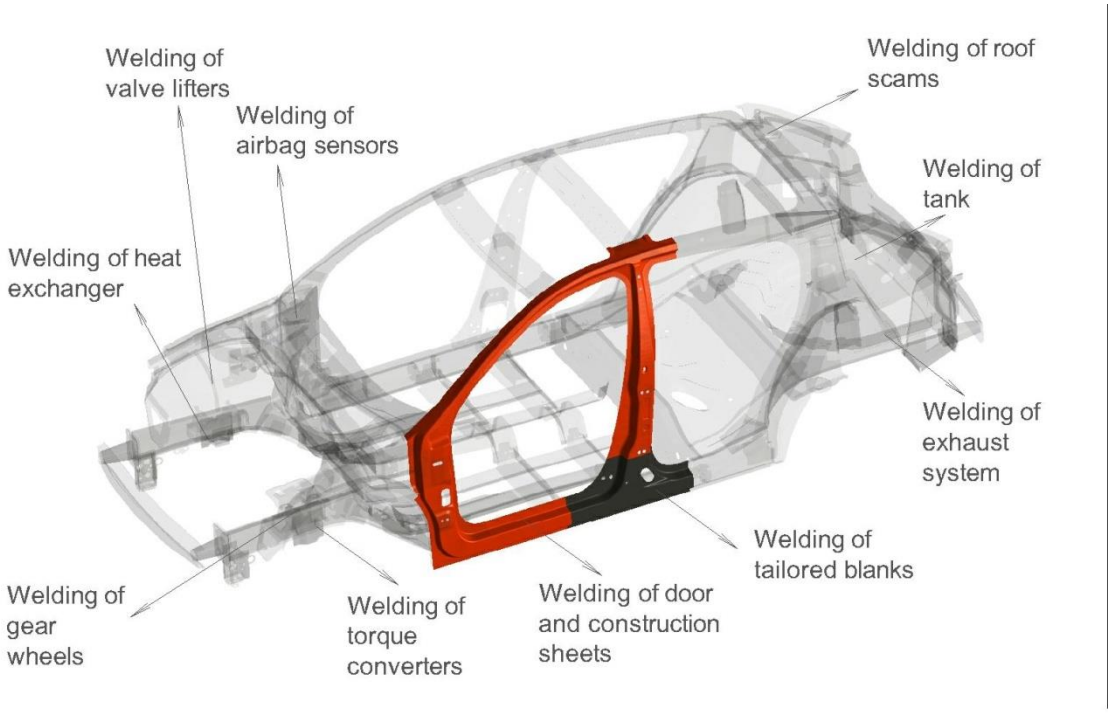

Figure 1.5. Some automobile applications.
(Source: Steen and Mazumder 2010)

In plastic processing:

9. Most thermoplastics can be welded by laser. During plastic welding by using the laser transmission welding method, two different types of thermoplastics are connected to one another. One part is the transparent plastic while the other component is the absorbent one as illustrated in Figure 1.6. With this method the laser beam penetrates the upper transparent plastic and reaches the absorbent one below it. The laser melts the surface of the absorbent plastic with heat transferred to transparent component. The point of this overlap welding is that the components are welded together without any

particle of both parts being released. An advantage of this laser process is the fact that heat is transferred locally. By this way, weld seams could be created in direct proximity for applications where the welding zone temperature is critical such as electronic components welding. For this method, joining pressure is essential therefore, a clamping tool also has to be used in the process (Russek et al. 2003).

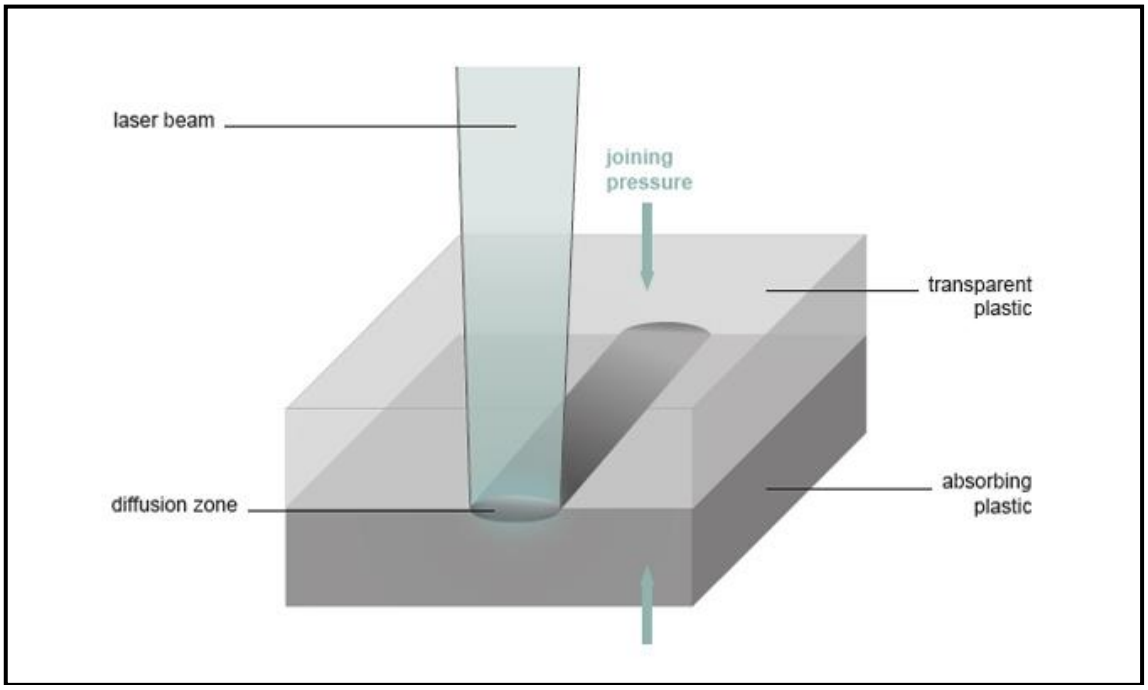

Figure 1.6. Laser welding of plastics.
(Source: Trumpf-laser)

In textile:

10. Welding of polymers and plastics – There are numerous and increasing number of applications for plastic welding. They include spectacles, diving suits, waders, outdoor footwear, tents, parachutes and soon carpets. For wetsuits, the process is to discharge polymer through a nozzle into which a 200W Nd:YAG laser beam is coupled in (Warwick and Gordon 2006). The beam gently heats the polymer and the joint area allowing the polymer to flow into the fabric. In the process, no toxic chemicals are used and this method is 100 times faster for making wetsuits than conventional methods for manufacturing wetsuits since the seam is finished in one pass without any extra passes, stitching or sealing (Steen and Mazumder 2010).

11. Smart garments – Consideration of saving labour costs, the manufacture of smart or advanced garments can be automated. Recent works on control and monitoring of such a process has been published. Smart or advanced garments could include smart elements based on electrical or optical phenomena by including electrical conductors or optical fibers in the fabric (Jones and Rudlin 2006).

In construction and architectural design parts:

12. Building shapes out of powder and wire – Deposition welding is a developed process that is applied for surface finishing which is for repairing or modifying existing components. In the case of manual deposition welding, the laser welder guides the filler material manually to the area to be welded. A thin wire with a diameter between 0.15 – 0.6 millimeters was primarily used as filler material in this process (Brueckner et al. 2011). The laser beam melts the wire. The molten materials form a strong bond with substrate, which is also melted, and then solidifies, leaving behind a small raised region. In the case of automated deposition welding, a machine guides the filler material to the area to be welded instead of an operator. Metal powders could be used primarily and applied in layers to a base material. The metal powder is fused to the material without any pores or cracks and forms a high-tensile weld joint with the surface. After cooling, generated metal layer can be processed mechanically. The strength of this process allows it to be used to build up a number of similar or different metal layers. Several powder coatings are melted onto one another or next to another as required. Figure 1.7 shows a coated surface by deposition welding.

Figure 1.7. A surface coating application.
(Source: Trumpf-laser)

In home appliances:

13. Heat conduction welding – In heat conduction laser welding, the laser beam melts the mating parts along a mutual joint. The molten materials flow together and solidify to form the weld (Figure 1.8). Other applications can be found in electronics. The laser produces a smooth, filled seam that does not require any other grinding or finishing. Pulsed and solid state lasers are used in such applications. Heat conductivity of welding materials defines maximum weld depth for this process. The depth of weld is always smaller than its width. Welding of cooker tops which is made of two stamped sheets is accomplished by using that method (Geiger et al. 2008).

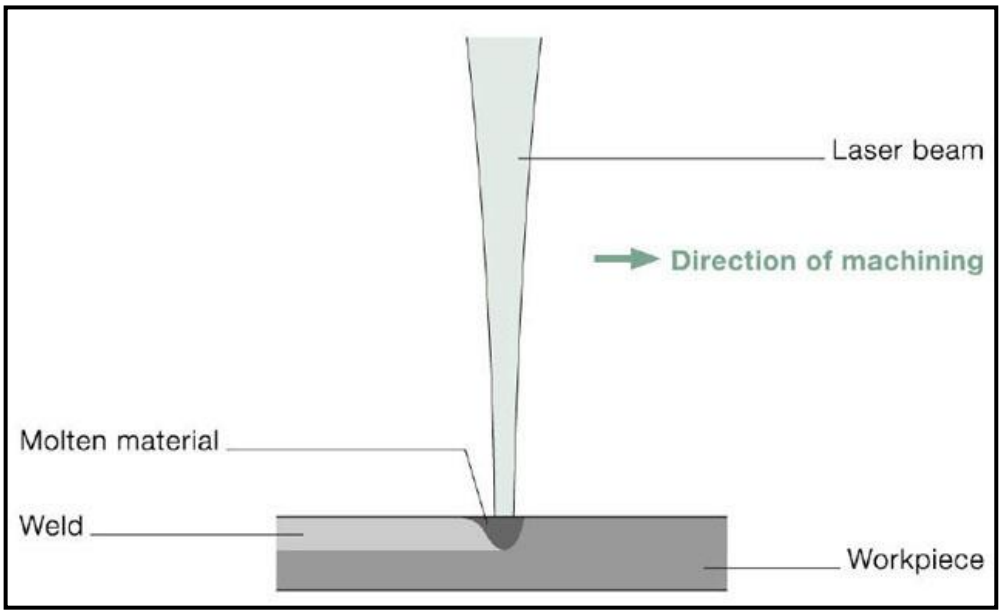

Figure 1.8. Heat conduction welding.
(Source: Trumpf-laser)

In marine:

14. Underwater laser welding is known as one of the best methods for deep-sea divers. It is difficult to maintain electric arc or flames at high pressures. The laser beam can be passed down a fiber for several kilometers. Some of the recent work shows that the process works and that shroud gas is not strictly necessary since the high-power beam makes its own keyhole through the surrounding water (Shannon et al. 2012).

In ship building:

15. By combining laser welding and one other welding technique, a steel construction can be achieved. Compatible processes are MIG (metal inert gas) or MAG (metal active gas) welding as well as TIG (tungsten inert gas) or plasma welding. Large steel plates that can be up to 20 mm thick are welded together. To overcome the big gap problem with respect to laser welding abilities, laser welding is combined with MIG welding. Laser delivers the high power densities needed for the deep welds and enables high welding speeds. By this primacy, laser welding reduces heat input and distortion. The MIG bridges the gap between the parts and welds the joint using filler wire. On the whole, the hybrid techniques are faster than MIG welding alone and the parts are exposed to less distortion (Pantsar et al 2001).

In heating:

16. Deep penetration welding – High power densities are applied to both materials that intersect each other. The materials are melted together during process. A molten pool of materials creates a keyhole, which is surrounded by melted materials. The molten substances flow around the keyhole and solidify in its trail (Figure 1.9). The laser beam is absorbed by both materials so the efficiency of the welding process rises that welding depths can reach up to 25 millimeters. Industrial type of heat exchangers and design radiators are often seen as a laser welding applications (Quintino et al. 2007).

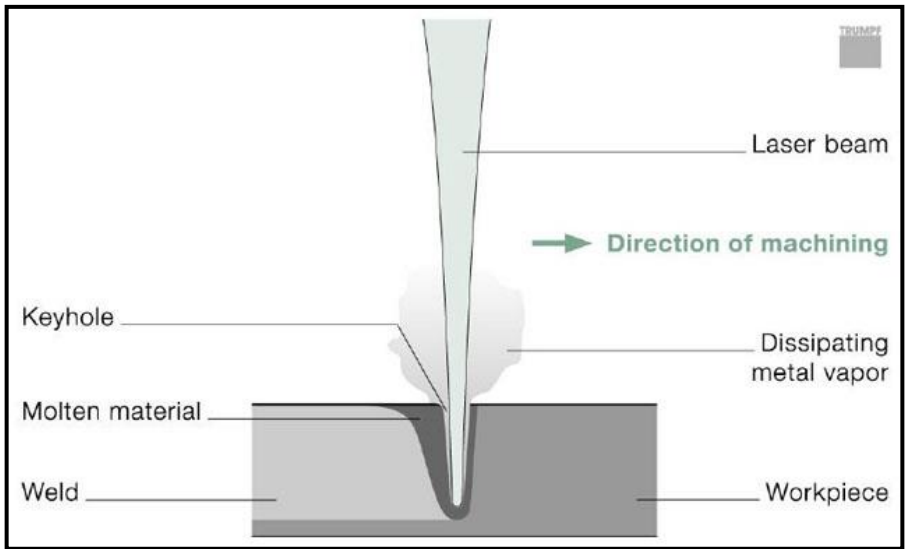

Figure 1.9. Deep penetration welding and keyhole.
(Source: Trumpf-laser)

In medical:

17. Surgery and medical engineering – Preparation of human albumin solder for laser tissue welding (Poppas et al. 2005).

Although laser welding finds application in many different types of industrial settings, there still remain open areas for improvement for laser welding process (Neto and Mendes 2013). One of the crucial areas of investigation is the control of the laser welding since it requires an automated process. In this thesis, the main investigation is on improving the monitoring and control of laser welding process to increase the quality of the process output. Aims of this study are further explained in the next section.

1.2. Aim of the Study

In industry, laser seam tracking systems are applied extensively. However, there are still unsolved problems such as the inability to track complex seam, the error of look-ahead detection and seam path identification for variable gap joints. In this thesis, the work carried on for laser welding seam path identification is presented. Through this identification, the aim is to monitor the laser welding process and correct the pre-described path to have an improved control of the process. For this aim, objective of this thesis is to develop a 2D vision based seam path modification technique and a computer aided design (CAD) based sequential measurement control to decrease possible welding faults. An industrial type of CCD (charge coupled device) camera is used for visual measurements. An operational interface is developed in order to make the process user friendly. As a result of seam path identification, modification codes are generated and sent to CNC (computer numerical control) machine. The experiments for the technique are implemented in an experimental test setup, which consists of a 1kW (kilowatt) solid state fiber laser, an industrial laser welding head, a CNC machine and a CCD camera.

1.3. Outline

The thesis consists of 6 chapters including Introduction, Literature Survey, Subsystems, Methodology, Test Results and Conclusions. Second chapter is reserved for presentation of surveys on challenges to implement path identification techniques and appropriate laser welding and sensing techniques for the industry. In addition, laser source types, laser welding sensing techniques for automation and welding parameters for different kind of materials are explained. In Chapter 3, applied technique and interactions of subsystems are reviewed with the help of a flowchart. Chapter 4 presents the main components of the system and the applied methodology for test setup. The image processing software and graphical user interfaces are presented at the last part of this chapter. In the following chapter, experiments and their results are provided. Efficiency of the technique and its repeatability is evaluated in this chapter. Based on the results of the study, discussions are made, conclusions are given and future works are addressed in the final chapter.

CHAPTER 2

LITERATURE SURVEY

After the principle of laser was described by Albert Einstein in 1917; this emitted light has been revolutionized by studies so far. The first optical fiber laser and its stimulated laser beam production within the optical fiber in a cavity were discovered in 1961 by E. Snitzer. In 1966, Alfred Kastler won the Nobel Prize for physics on optical pumping of a laser beam (Nobel Prizes of Physics 1966). First industrial opportunity was created for lasers with the application of cutting a 2.5 mm thick stainless steel plate at a 1 meter/min under dioxygen with a 300 W power CO_2 laser with a first laser cutting optical head (Sullivan and Houlcroft 1967). In subsequent years, researches were performed on materials for fiber optics and stimulation methods for low-power fiber lasers to produce high quality and reliable light. After 1980s, the CO_2 laser use decreased. Fiber lasers have started their comeback since the development of ultralow loss fibers for communication (Diels and Arissian 2011). In 1990s, with the rapid growth in the telecommunication sector, use of fibers in a fiber optic network for high amount of data transfer increased rapidly. Due to the crisis in the telecommunication sector, the industrial production and research were shifted towards high power fiber lasers to be used, so in the beginning of 2000s, high power fiber lasers whose capacities reach to KW levels started to be used (Injeyan and Goodno 2011). After 2010, demands for industrial laser systems has increased rapidly again. Research between 2000 and 2010 reflected to the marketing of laser systems and fiber lasers, which comprise %70 of industrial applications in the field of metal machining, and fiber laser welding constitutes %25 of the market in the recent years (Belforte 2011). As a result of quick evolution of fiber lasers in industrial application, practice-oriented experience and know-how have significant importance and still limited sources in the market.

2.1. Laser Sources

"Laser" is the word is an abbreviation for "Light Amplification by Stimulated Emission of Radiation". Laser wavelengths extend from the wavelength of infrared (IR) to ultraviolet (UV) and are formed by both of extending light intensity and composed of a single frequency and inphase radiation beam. Therefore, laser systems have a longer emission range without any loss with respect to other rays (Csele 2004).

A laser beam is achieved by an external given inhibitory effect on a substance for providing photon emission around. Some of the emitted photons that are reflected from the surface of substances crash to container's reflective inner boundary and cause to a spread of new photons. As a result of continuing chain reaction, inphase and monochromatic laser beam occurs in the container. The beam with the help of an optically transparent hole on the surrounding container is routed from container to required directions.

The essential external energy source for generating a laser beam is generally transmitted by a chemical, electrical or an optical source. Today, lamps and diodes for solid state lasers (Nd:YAG and Ytterbium Fiber) and high frequency electricity sources for CO_2 lasers are known as the most common inducers in the industry (Chang 2005).

Container of substances which emits the laser beam can be manufactured in different ways. For gas lasers, it is made to prevent leakage of gas and consists of metal or glass tubes which are formed of a complete reflective mirror on one side and centered fully or semi permeable reflective mirror on the other side. Thus, the gas could be induced twice by the reflected laser beams from the mirrors and emission of laser could be occurred efficiently by the permeable region of the mirror. For solid state lasers, as crystalline in shape varies, laser type changes respectively (rod, fiber or thin disc, etc). The crystalline is stimulated within the container with one or more points supplied from stimulating light beam and emitted laser beam by this way. Fiber lasers transmit the laser beam by a protective and stimulated covering, which covers a tube consisting of particles with a few hundred micron diameter of crystalline. Whereby, produced laser beam can only ray one way by isolating one side of fiber tube. Fiber optic cables can transmit the laser beam to the destination point by connecting the open side fiber tube (Ion 2005).

In the industrial area, different laser beam generation techniques are in use. Techniques are separated based on beam generation types, wavelengths, maintenance, power efficiency, cooling loads and life (Steen and Mazumder 2010). Commonly used industrial lasers for welding are discussed below.

2.1.1. Solid-State Lasers

First developed solid-state laser is ruby laser. Ruby is aluminum crystalline that contains small amount of chromium. Red laser beam is emitted by these chromium atoms (Csele 2004).

With the development of another solid-state laser; Nd:YAG, the use of solid state lasers has increased rapidly. In this laser type, cylindrical rod-shaped crystals are coated with an antireflective substance and two ends of the rod are polished. The crystals are fixed in a metal container. Depending on method that is applied as stimulus, special flash lamps and reflective mirrors are placed into the container. The stimulated Nd:YAG crystal by a high energy light generates a laser beam with a wavelength of 1064nm (Koechner and Bass 2003).

The most important problem in this type of lasers is thermal stresses that are formed between the inner and the outer surface of induced crystalline as a result of temperature variations. These thermal stresses affect the crystalline structure in terms of limiting emission of laser beam quantity and quality. As a solution to this problem, instead of using a cylindrical rod-shaped crystal, a thin disc or a long and thin fiber form is studied to produce a laser beam. As a result of these studies, more efficient disc and fiber lasers have been developed and better laser beam quality is provided. In such crystals, distance between the stimulation surface and the interior of the crystal is lower than a few hundred microns so the significant thermal stress on the crystal structure is not occurred. By this method, the crystal is used more efficiently (Koechner and Bass 2003).

Pumping is the process by which atoms are raised from a lower to a higher level energy to emit a photon. For solid-state lasers, pumping is commonly done by using a flash lamp or a diode. A lamp-based optical pump produces a spectrum of light which causes most of the energy to be wasted as heat. Also, these pumps have shorter lifetime than diode pumps (Kannatey-Asibu 2009). A diode-based pumping laser infuses energy

at a specific wavelength so a small amount of energy is wasted. The diode pumps are used mainly because:

- They have a relatively high efficiency, which results in a reduced electrical power consumption for a given desired output power,
- They can generate high output power,
- They are available in many wavelengths, which means they can be a solution for different application demands,
- They require reduced maintenance. The working life of diode-pumped lasers is generally more than 12,000 hours, while that for lamp-pumped lasers in the range of 600-1000 hours,
- They are much smaller in size (Kannatey-Asibu 2009, Koechner and Bass 2003).

There is a summary on solid-state lasers below:

Nd:YAG laser: Nd:YAG lasers use Neodymium (Nd) diffused in a crystal that is composed of yttrium aluminum garnet (YAG) to produce a light beam. Nd:YAG lasers emit a wavelength of 1064 nm, which is near infrared. These lasers are exactly ten times smaller than CO2 lasers. Due to their small wavelength, Nd:YAG lasers are primarily used on metals and cannot be absorbed by organic materials like glass and plastics (Kannatey-Asibu 2009, Csele 2004).

Fiber Laser: Fiber lasers use rare-earth elements such as erbium, ytterbium, neodymium, dysprosium, praseodymium and thulium. Fiber lasers emit wavelength of approximately 1064 nm as Nd:YAG but higher electrical energy efficiency which reaches more than %30. They are compact and electricity is the only consumable cost (Kannatey-Asibu 2009, Csele 2004).

2.1.2. Gas Lasers

Gas lasers produce laser beam by inducing gaseous substances. These substances are placed into a sealed tube and fixed and then the laser beam is stimulated through the electrodes which are fixed in various regions of the tube. Depending on the type of laser used, gas mixture varies. In the first gas lasers, helium and neon was used as a mixture. Subsequent studies on gas mixture are presented that mixtures of CO_2

lasers are more efficient than the helium and neon lasers. These lasers are used commonly for industrial processing due to wavelength of laser beam they produce and high power capacities (up to 50 kW) (Csele 2004). In time, studies are directed towards new closed type lasers which do not require a gas feed during process. These type of lasers have compact structure and their operating costs are lower than CO_2 lasers that required gas feed. Generated heat in the closed laser tube is transferred to the outer surfaces by help of the mixture gas. CO_2 lasers are widely used in the processing of plastic materials.

When the CO_2 lasers are in use of high power levels (>1 kW), high speed gas circulation for cooling is needed due to overheating problem of the gas within the tube so a high level output and fast gas flow rate within the tube have to be provided by a complex turbine pump. These complex chillers increase the risk failure as well as the cost of the process (Kannatey-Asibu 2009).

Electrical-based laser pumping is more commonly used with gas lasers. The narrow absorption bands of gas lasers make them less convenient for optical pumping because optical pumping is a broad band energy source in most cases and only a small fraction of the released energy would be absorbed by the narrow band gas, making the process inefficient. Thus the gas lasers are normally pumped electrically (Kannatey-Asibu 2009).

CO_2 laser: A CO_2 laser is a gas laser, which uses Carbon Dioxide, CO_2, as a medium to produce the infrared light. They emit a wavelength of 10600 nm, which produces an intense infrared light. CO_2 lasers are easily absorbed by organic materials, for example plastics, glass, fabrics and acrylics (Kannatey-Asibu 2009, Csele 2004)

2.1.3. Semiconductor (Diode) Lasers

This type of laser is made by crystals obtained from the semiconductor materials. Gallium arsenide crystal is one example of a semiconductor material. The electrons lose energy and emit photons when positive voltage is given “p” side and negative one is given “n” side on combination surface of “p” and “n” type materials in this kind of crystal lasers. This photon-electron collision provides more photon production. As a result of photons reaching an adequate level composes laser beam (Weber 2001). These lasers are efficient source of light. Semi conductive lasers work

with more than 50% efficiency. Wavelength and optical characteristics of laser beam, which is produced by diode lasers, are widely used for industry, metal and plastic materials welding, and several numbers of surface processes such as surface hardening, surface cleaning (Chow and Koch 1999).

Diode lasers have high power intensity, which is distributed regularly to laser spot area. The spot area can be square, circular, rectangular or diamond shaped optionally as shown in Figure 2.2. This option makes them a powerful solution for heat treatment and seam welding applications where a regional power density is required. However, that featured output requires an additional focusing process for cutting and deep penetration welding (Laserlines 2014). Companies want their laser source to use both in cutting and deep penetration welding operations which require focused laser beam (Gaussian Output). To meet customer demands for both cutting and welding applications, diode laser technology still cannot provide a solution for these requirements. Therefore, diode lasers are not used in comparison table that is illustrated in Table 2.1.

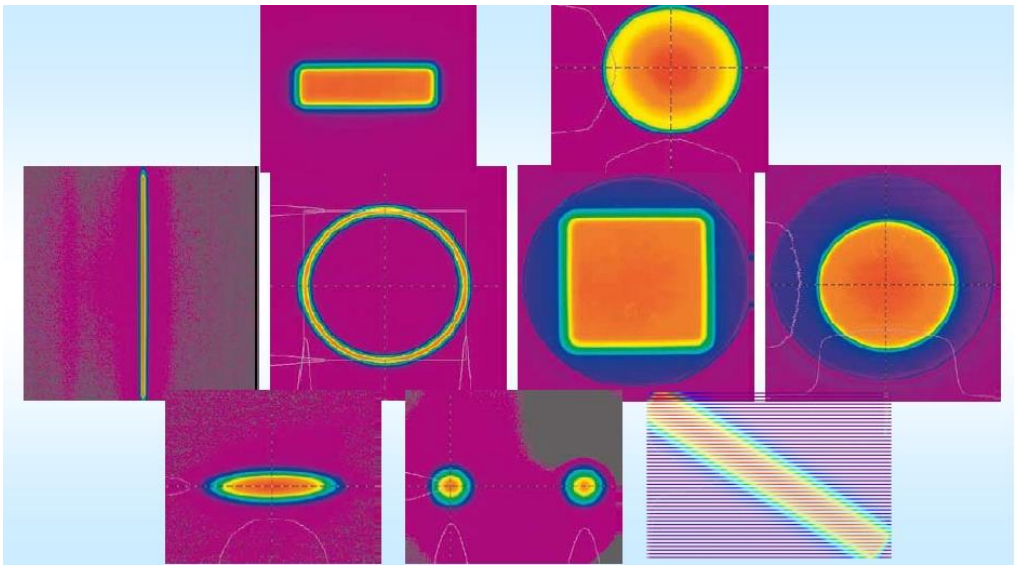

Figure 2.1. Diode laser spot shapes.
(Source: Laserlines)

Solid state lasers and gas lasers react very differently on different materials because of the differing wavelengths of the laser beams. The wavelength of a YAG

laser (1064 nm) is exactly ten times smaller than the CO_2 wavelength of 10640 nm, which makes it ideally suited for absorption in most metals, but this small wavelength inhibits its ability to be absorbed by many other materials (wood, acrylic, plastics, fabrics, etc.) (Steen and Mazumder 2010).

A comparison table between lasers that are used for laser welding operations in industrial field is listed in Table 2.1 by considering pump method, wavelength, maintenance, power efficiency, cooling load for 2 kW and life.

Table 2.1. Comparison of Industrial Type Laser.

	Fiber Laser	**Nd: YAG Laser**	**CO2 Laser**
Pump method	Diode pumped	Lamp and Diode pumped	Lamp pumped (amplified by CO2)
Wavelength	1064 nm	1060-1200 nm	9400-10600 nm
Maintenance	No maintenance	Frequent adjustment, optimized power output, periodic change of lamps/diodes	Change purge gas (35.000$ per year)
Power Efficiency	170 W per hour Up to %50	6 kW per hour %2-3	700 W per hour %10
Cooling for (2 kW)	20.000 BTU	200.000 BTU	100.000 BTU
Life	50.000 – 100.000 hours	1000 hours (lamp) 20.000 hours (diode)	20.000 hours

Laser outputs are in two wave types:

- Continuous wave (CW) – where the output power is essential
- Pulsed wave (PW) – where the output power varies

The CW output is used more than the PW output. However, the PW output has advantages in a situation when variation of the on/off ratio or duty cycle of the pulsed beam enables applications such as drilling and cutting. The reduced heat input also creates an advantage for pulsed suitable parts that are sensitive to distortion. However, lower overall power results in a reduced processing speed (Kannatey-Asibu 2009). In processes such as seam welding, where there is a need for continuity and stability, the CW output is suitable.

In this study, complying with the low laser wavelength, continuous wave output and low chiller load requirements, a 1kW fiber laser is used in experimental setup.

2.2. Importance of Laser Welding Automation

The laser welding task in steel-sheets is difficult due to limited workspace and path identification. Therefore, many efforts have been spent for automation. The main challenge for automation is the development of simple and well-defined seam identification algorithm that can be applied to a robotic welding application (Chang et al. 2011).

Despite the performance of laser welding, the process requires high level human and environmental health and safety precautions. These needs generate challenging engineering problems to develop an advanced automatic manufacturing process without any human intervention. Beyond research for an automation system, no exact model has been defined so far since the process itself is complicated. For improved automation of the process, an adaptive control system has to achieve a real time measurement in order to control welding parameters. This might enable prediction for possible defects (Xiadong 2010).

For fully automated systems, manufacturing processes should be controlled by acquiring sufficient process data through necessary sensors to adjust welding parameters in real-time. Welding automation industry focused on the control of the laser welding process and developed control solutions by customized closed-loop control algorithms, which increase product quality and optimize existing manufacturing systems. Adaptive control is a possible solution for this process (Norman et al. 2007). Another possibility is the use of neural network, which learns the effects of dynamically changing welding parameters through the data acquired from a group of sensors (Sun and Kannatey-Asibu 2002, Bad'yanov 2003). The implementation of these types of new control systems is a necessity for entirely novel processing techniques (Fraunhofer 2011).

2.3. Monitoring Techniques

In the last decade, use of laser welding monitoring and inspection of laser welding processes are increased. Studies rely on complex signal processing and sensing techniques such as optical, visual, acoustic and thermal variations (Shao and Yan 2005).

High energy density of laser welding process generates material interactions due to emission energy in a variety of forms, optical and acoustic emissions are one of these forms. These process feedback signals can be obtained by using suitable sensors. The signals contain a laser welding process information about defects. Therefore, these signals can be used for online control of welding parameters. Also, laser beam that is not absorbed is reflected to environment as a radiation as shown in Figure 2.3. Acoustic emissions are generated from the stress waves induced by the variations of internal structure of a workpiece (Figure 2.3). For instance, The surface radiation is in the visible and infrared range for Nd:YAG laser spot welding (Ostendorf et al. 2003). In CO_2 laser deep penetration keyhole welding, the plasma generates an emission light with a wavelength between 190nm and 400nm and the spatter emits light between 1000nm-1600nm wavelengths (Ono et al. 1992). Furthermore, geometric parameters of the keyhole and melt pool, represented in Figure 2.3, contain information which is acquired by a vision sensor (Shao and Yan 2005).

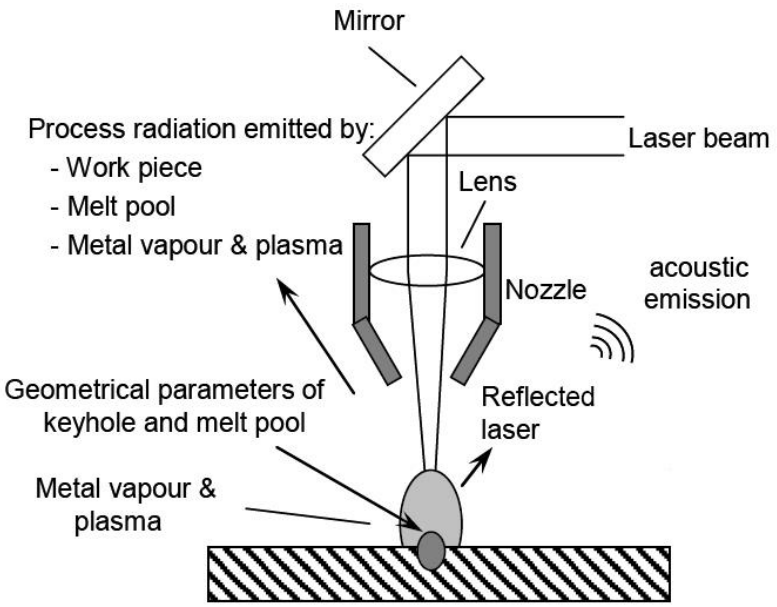

Figure 2.2. Detectable signals during laser welding.
(Source: Shao and Yan 2005)

2.3.1. Acoustic Emission Technique

The technique involves a sensor which collects process sounds and converts them into an electrical output to be used as a controlled variable. Typical sensor for this emission is a microphone which is placed nearby the weld zone.

The application of acoustic emission has been reported to be used in the monitoring and characterization of laser material processing by Li et al. (1996). A piezoelectric sensor is used to capture any acoustic mirror signal from under the workpiece. The signal is generated by the back-reflected laser signal and processed to describe the emission and welding performance (Li 2002). A frequency response is obtained between 20 kHz and 0.5 MHz to investigate resonant relationship during laser welding of metals by Gu et al. (1996). By considering the emission ranges of the process, changes of welding parameters and results are presented by Shao and Yan (2005) in their work.

Acoustic emission techniques are still researched in academy. However, the number of applications of this method is decreased due to their limitations. Better control algorithm for monitoring and contact installation of sensors is needed and the technique is not suitable for mass production because of noisy environments in industry. Another disadvantage of the method is its limit while detecting difference of partial penetration and full penetration.

2.3.2. Photodiode-based Optical Detection

The emitted radiation from welding process is converted into an electrical signal by a sensor. An optical filter is placed in front of the sensor to limit the data acquisition ranges of the whole sensor system. Process is particularly detected in ultraviolet (UV) or infrared (IR) ranges. A typical setup is illustrated in Figure 2.4.

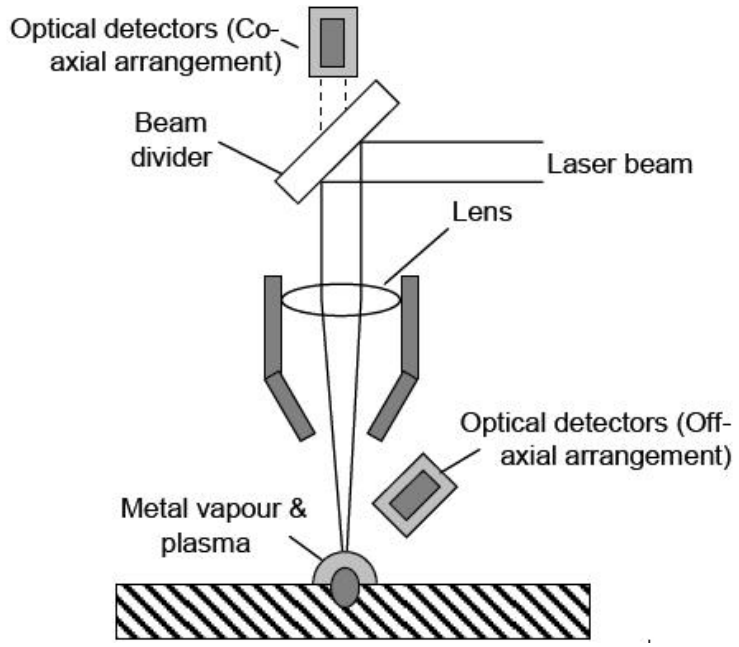

Figure 2.3. Photodiode based optical sensing.
(Source: Shao and Yan 2005)

A photodiode based optical sensor detects plasma plume emission and thermal radiation of the weld pool. The measurements have relation between penetration depth and emission intensity. Studies on optical signal sensor design have been carried out (Ostendorf et al. 2003, Ostendorf and Temme 2004, Tönshoff et al. 1998, Park and Rhee 1999, Park et al. 2002, Sforza and Blasiis 2002). Dynamic plasma intensity was sensed with a silicone photodiode with a preamplifier.

Similar study, which was based on ultraviolet and infrared photodiode, was accomplished by Park et al. (2002). In that work, a CO_2 laser welding process was measured by using photodiode sensors. Acquired data from the plasma and metal vapor was used to describe a relationship between the heat distribution and the emission.

Another experimental study is based on evaluation of the laser welding quality under classification of heat input, slightly low heat input, low heat input and partial joining due to gap mismatch. Welding quality measurements were resulted with a complete and partial joining. To define influence relationship between welding parameters and emission of plasma and spatter, a fuzzy logic multiple signal processing analysis and neural network estimation method for penetration depth and width was achieved. (Park and Rhee 1999, Park et al. 2002) Furthermore, underwater laser welding quality monitoring to detect the IR and UV waveband of optical emission was

studied and various shielding conditions have been presented (Zhang et al. 2004, Sforza and Blasiis 2002).

If a co-axial measurement was to be implemented, a beam divider (dicroic mirror) was used for sensing. Tönshoff developed an online process monitoring system where the sensor was installed using the co-axial arrangement (Tönshoff et al. 1998).

Another technique which contains both photodiode and pyrometer was defined by Bertrand and Greyey (2000). To monitor surface temperature of welding zone a multi-wavelength pyrometer was used so that process parameters can be measured. They carry out to identification of temperature variation with operational parameters and detect possible welding defects for Nd:YAG continuous laser welding.

Photodiode based optical sensing is easy to implement and low cost. However, it is not immune to system noises that result in poor accuracy.

2.3.3. Vision-based Keyhole Geometry Sensing

During laser welding process, high energy intensity is focused on a position and a keyhole is created around molten pool. Keyhole shape and geometry information can be used to detect penetration depth or possible welding defects such as pores and cracks. Important point for this technique is that a small heated zone can be controlled and results in better after-work quality compared to mentioned techniques above.

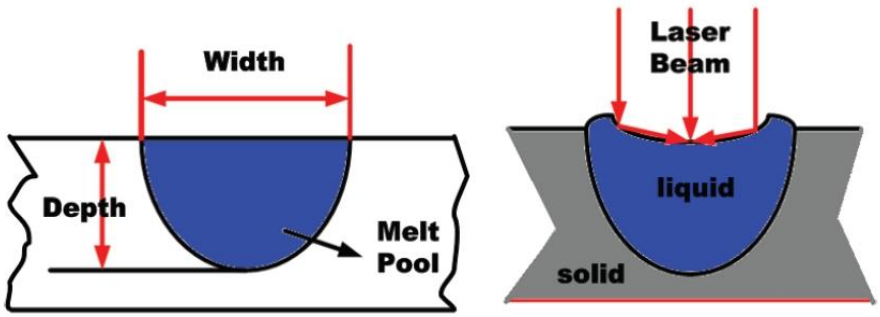

Figure 2.4. Keyhole geometry identification.

The keyhole geometry information contains weld pool width and depth data as shown in Figure 2.5. The images, which are acquired with CCD or CMOS cameras, are studied to define a relation between various parameters such as speed, laser power and

pool geometry. Advanced optic filters are used to measure the images due to high contrast microstructure of laser welding process (Kannatey-Asibu 2009). Online and offline control loops are developed so that whole system can adjust welding parameters with respect to sensed data. Farson (1999) developed a successful 2D and 3D measurement system that provides required welding pool geometry and control performance. A compact filtered camera system has been developed to measure the planar geometric size of weld pool. A system for a closed-loop control and laser welding monitoring based on CCD-CMOS camera was published by Na et al. (2010). Investigations for geometrical parameters of the keyhole are still being researched.

Observation of melt pool and keyhole geometry was carried out to determine gaps between molten sheets for industrial applications (Shao and Yan 2005). A robust image processing for edge detection and evaluation was made for 1 kW Nd:YAG laser by help of a 500 frame per second CMOS camera. It was observed that as the gap gets smaller, the melt pool width decreases and pool length increases (Kairle 2008).

2.3.4. Pre-process Sensing Techniques

Besides whole in-process sensing techniques presented above, an automated laser welding process calls for a well-defined seam path and workpiece-joint due to small size of focused laser beam on workpiece. Therefore, the process permits only a limited gap between the two joining parts. If parts are too far apart from each other, that means there is insufficient weld material to bridge the gap and the welding process will result in an undercut defect. For an acceptable result, the gap has to be zero or with an allowable gap since a zero gap is not practically possible. An allowed gap should never be more than %10 of thinnest material (Unitek 2003).

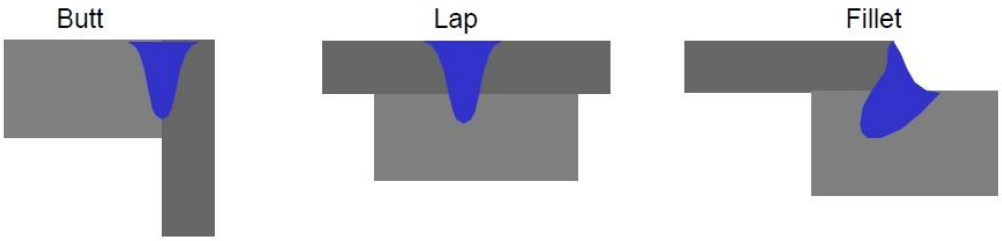

Figure 2.5. Most common weld joints.
(Source: Miyachiamerica 2014)

The part alignment with respect to laser beam direction is another important point for pre-processing. Focused laser size on workpiece (spot size) varies between 100 to 1000 microns for laser welding applications. For a deeper penetration, a smaller spot diameter is required. The alignment of the joint under laser beam for different types of weld joints (Figure 2.6) must be precise enough so that the focused spot does not go off the track of the joint path. The tolerance of the alignment is given as a function of spot size diameter in Figure 2.7 (Unitek 2003).

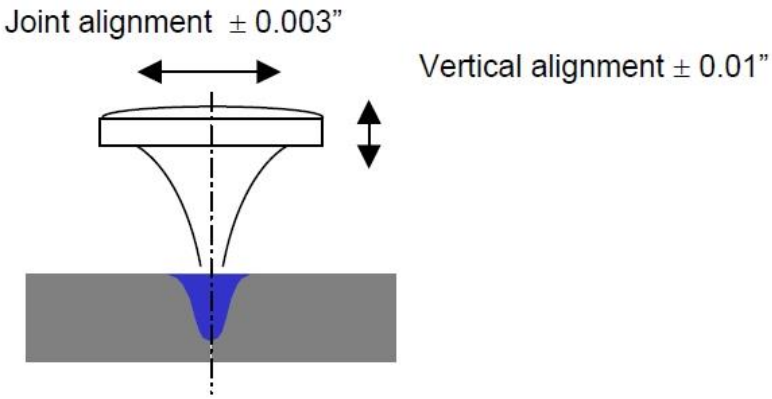

Figure 2.6. Laser beam alignment tolerance.
(Source: Miyachiamerica 2014)

When in-process sensing techniques are considered with respect to the pre-processing needs, the required distance between the laser welding head and workpiece, which is called as focal distance, have to be defined properly to adjust the spot size. The focal distance limits all of the in-process measurements. To inspect the quality of the laser welding, the measurements on high penetration depth and joining definition of workpieces are the key aspects. Adaptive systems only detect changes of welding parameters with respect to acquisition data, which is provided by different type of sensors. However, no distinct correlation algorithm between the laser source and sensor-based information is defined for real-time laser welding control systems. Therefore, the pre-processing techniques such as positioning of workpiece, seam path identification and seam tracking are possible solutions in the condition that they should be based on accumulation of enough practical information on the effects of welding parameters. The use of such techniques has become a common practice in order to achieve optimum weld quality (Kairle 2008).

All pre-processing techniques depend on sequential measurements that detect initial-terminal points of weld trajectory, seam geometry and gap distance by use of a vision sensor. Studies start with determination of a workpiece location with respect to welding torch (Smith and Lucas 1989). Then gap inspection method and workpiece alignment technique was applied to butt-joint mild steel welding by using CO_2 laser by Jeng et al. (2000). With the increased computing speeds, seam tracking systems were able to measure the seam path in real time. A vision camera sensing seam tracking system was developed for a plasma arc welding which detects seam deviation to adjust the workpiece position adaptively to the sensed seam position by Ge et al. (2005). Another seam tracking system with visual sensing free from calibration for robot was applied to a gas tungsten arc welding in the work of Shen et al. (2010). A passive vision sensor (vision sensor imaging without any light source) based seam tracking method was published on Aluminum alloy pulsed gas tungsten arc welding (GTAW) (Xu et al. 2012). In this work, the experiments were not reliable due to simple welding path and the system was not compatible with the other seam tracking environments where different materials were used such as steel, steel-alloy. In recent years, a stereo vision algorithm was published for weld seam identification on robotic arc welding but only one millimeter precision for 3D Cartesian coordinates was achieved (Dinham and Fang 2013).

In industry, laser seam tracking systems need further improvements since the systems have weaknesses such as the inability to track complex seam and the error in look-ahead detection, which depends on the speed of welding. To overcome such problems, a CCD vision camera and CAD data based positioning method to verify vision data for machine position is used in the experimental study of this thesis.

2.4. Welding Defects Classification and Reasons

Beyond the high dynamics of laser welding, automation challenges, small size of process zone and modelling difficulties result in several welding defects. Experimental studies suffer from insufficient welding parameters knowledge for every new type of laser welding application. Therefore, the laser welding process and reasons for defects are not understood or modeled with enough precision.

The defects directly influence safety and mechanical performance of the final product. Despite a small size of heat affected zone and high energy density, complexity of system, misalignment of workpiece or wrong welding parameter choice result in different failures such as lack of fusion, lack of penetration, blow-out hole, crack, undercut, pores and voids. The defects are classified into three types, as shown in Figure 2.8, with respect to their related reasons; geometry related, applied process related and metallurgical related.

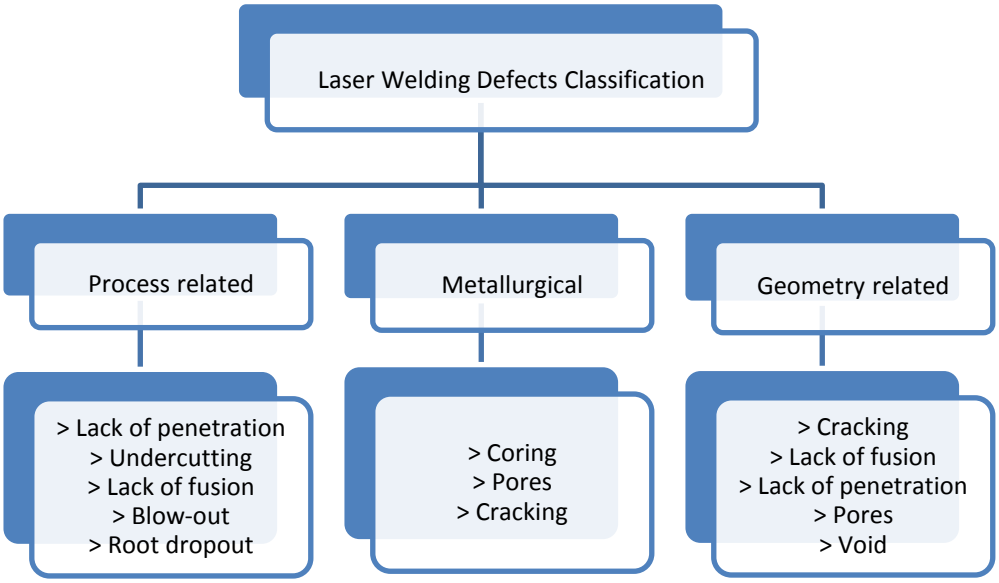

Figure 2.7. Classification of welding defects.

Currently, these defects are under research to improve the efficiency of laser welding in the industry. Mechanical properties of the welded parts should satisfy customer demands. Therefore, failures and physical causes of these failures have to be classified so that they can be controlled. The physical causes of defects are presented in Table 2.2 and Figure 2.9 (Kannatey-Asibu 2009).

Table 2.2. Explanation of laser welding defects and their physical causes.
(Source: Norman et al. 2007)

Defect	**Explanation of the physical cause**
Pore	Spherical gas bubble trapped by solidifying material
Blow-out	Caused by a near surface pore that opens and forms a crater
Cracking (hot/cold)	How cracks are formed during solidifying in welded zone Cold cracks can form after welding, often in heat affected zone
Void	Sharp edged geometry caused (volume) by impurities of during resolidification
Undercut	Not enough material in upper weld zone, depends on speed, power and gap
Lack of penetration	Joint not completely penetrated, depends on oxidation, gas protection, contamination of gas or fluctuation of laser power
Reinforcement	Too much material in upper weld zone, fluctuation of gap width
Root dropout	Too much molten material in lower weld zone

Vision systems along with new algorithms are used for monitoring welding quality in terms of detected defects after welding. Welding profile along the seam was used to identify surface failures such as cracks, undercut, reinforcement, root dropout, misalignment of welded sheets by Jeng et al. (2000). A vision algorithm was developed to detect cracks automatically during gas pipeline welding (Shafeek et al. 2007). Laser-based vision system with triangulation method was used to measure welding profile by Huang and Kovacevic (2011). In their work, a laser-based vision system was used to image 3D profile of welding zone. In this work, also, a comparison table of vision based quality inspection systems with respect to their initial cost, accuracy and data acquisition speed was presented.

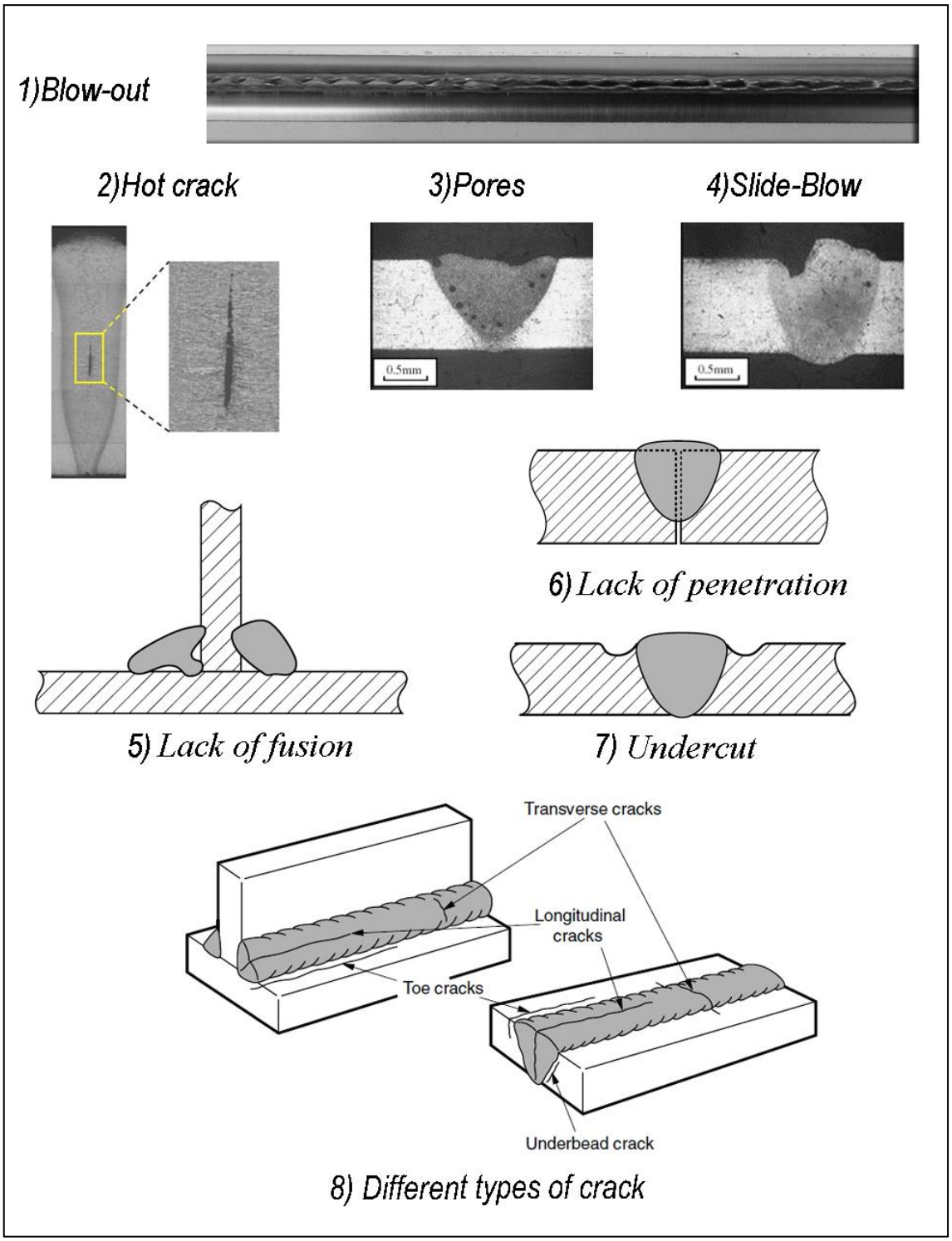

Figure 2.8. A visualization of welding defects.
(Source: Kannatey-Asibu 2009, Norman et al. 2007)

Detecting welding defects by using non-destructive methods bring up some limitations when vision based inspection systems are used. The applications of vision systems can only detect external defects such as reinforcement, blow-out, undercut.

Furthermore, the measurement accuracy of inspection systems increases from 0.01mm to 0.5 mm with respect to their initial cost. Furthermore, the systems are not compatible with real-time process techniques because transferred processing data is too large for USB information transfer capacity (Huang and Kovacevic, 2011). Despite these disadvantages, laser welding is a high-efficient and fast manufacturing technique when suitable parameters are applied during the process. If appropriate welding parameters are selected, the laser welding process quality can be improved. As a result of observations on various types of applications, companies that use laser welding increased their experience in defining welding parameters. An example work from the industry on a specific application and setting welding parameters for this application is presented for 1kW fiber laser for commonly used ss-304 and mild steel, Al-1050-H14 materials in industrial environment (Püskülcü and Koçlular, 2009). Next section is about applied welding parameters for the above mentioned materials.

2.5. Laser Welding Parameters

In laser welding operation, distribution of high energy density on materials evenly is the main purpose. To conform this purpose, setting laser power and speed is not enough alone. Focal position of laser head or shielding gas flow rate has to be adjusted to increase welding quality. The main parameters are discussed below:

- Laser beam power and welding speed
- Shielding gas
- Focal distance (between laser head and workpiece)
- Joint configuration
- Beam characteristics

Laser power and speed: Power and speed are primary adjustable parameters of laser welding process since penetration depth is affected directly with change of these parameters. The depth of penetration decreases exponentially with increasing speed. An experiment was presented by Kannatey-Asibu (2009) for use of 1700 W CO_2 laser on low carbon steel sheets. In this work, speed varies between 2500-7500 mm/min with the power change between 600-5000 W. Penetration depth results are illustrated in Figure 2.10.

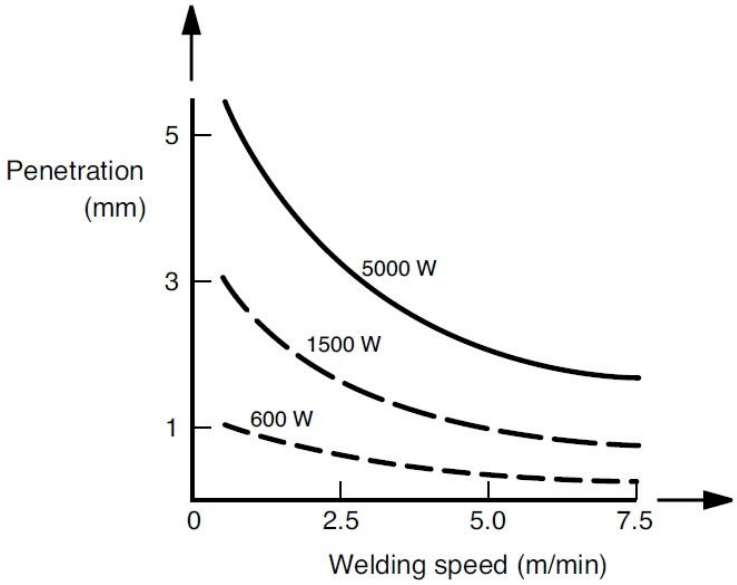

Figure 2.9. Effect of welding speed and laser power on weld penetration. (Source: Kannatey-Asibu 2009)

For a desired penetration depth, when a constant speed (feed-rate) is given, the input power has to be changed. However, low-power laser welding experiments (up to 5 kW) show that a 2 kW power cannot be extrapolated to 20 kW due to differences caused by plasma shielding effect. High evaporation rates cause enhanced plasma formation which absorb laser beam energy and radiate it to all directions. The radiated laser beam generates a plasma cloud with vaporized welding pool, which also can induce an optical effect that changes absorption of focused laser beam (Kannatey-Asibu 2009).

Shielding gas: In laser welding, shielding gas has more than one purpose:

- To blow away the plasma cloud and enable laser beam to reach on workpiece efficiently,
- To protect molten welding pool from environment effects,
- To protect laser head focusing lens.

Common gases for industrial use are Argon, Nitrogen and Helium. Argon is preferred more for low-medium power lasers because it is cheaper than Helium and its shielding results are better in higher density. However, Helium is used for high-power applications due to higher ionization potential, which means energy necessity for generation of plasma is higher than Argon for shielding (Figure 2.11). This allows more efficient absorption for reached laser beam to workpiece due to lower amount of plasma

formation. Also plasma formation is less significant when welding with a fiber laser, which is more efficiently absorbed than CO_2 and Nd:YAG at metallic surfaces while less is absorbed by the plasma. With a given set of conditions, penetration quality decreases from Helium to Nitrogen and Argon (Kannatey-Asibu 2009).

Fast emission of vapor from keyhole during welding causes shielding gas penetration through the keyhole. The formed plasma above keyhole with shielding gas is absorbed by molten pool so ionization potential of gases directly affects welding quality and this effect is getting higher and clearer at low welding speed and higher laser power conditions because of increasing vapor density (Steen and Mazumder 2010).

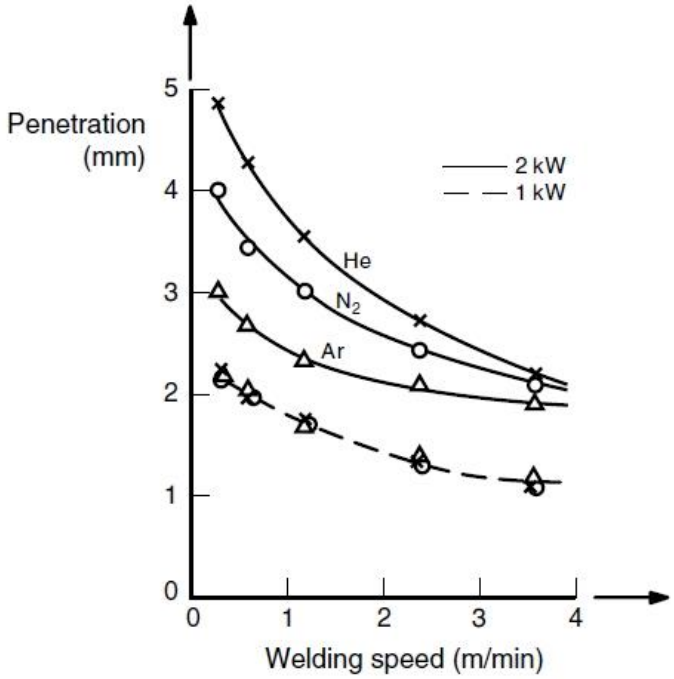

Figure 2.10. Shielding gas effect with laser power, speed and penetration depth. (Steel, Shielding gas flow rate: 20 L/min.) (Source: Beyer et al 1988)

Design of shielding gas blowers is another important parameter for total protection of molten pool. An illustration of the shielding gas blower setup is shown in Figure 2.12. Furthermore, flow rate of gases may cause waves on weld or side jets which blow the plasma and molten pool away from welding zone. Experiments done by Watson et al. (1985) have shown that blower position (or suppression jet) between 30-

60 degrees does not have an important effect but the increased distance between the workpiece and suppression jet decreases penetration depth.

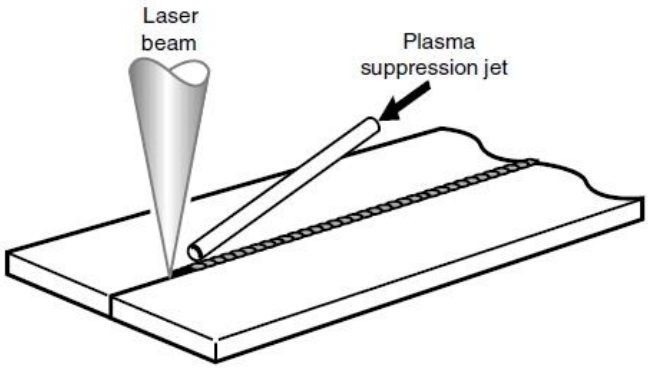

Figure 2.11. Shielding gas blower setup.
(Source: Kannatey-Asibu 2009)

With the increasing gas flow-rate, experiments indicate that beyond 40 L/min gas flow-rate is too high for keeping the molten metal on the weld pool and a transition appears until keyhole formation occurs with the increasing gas flow-rate. The effect of shielding gas flow-rate on penetration is illustrated in Figure 2.13.

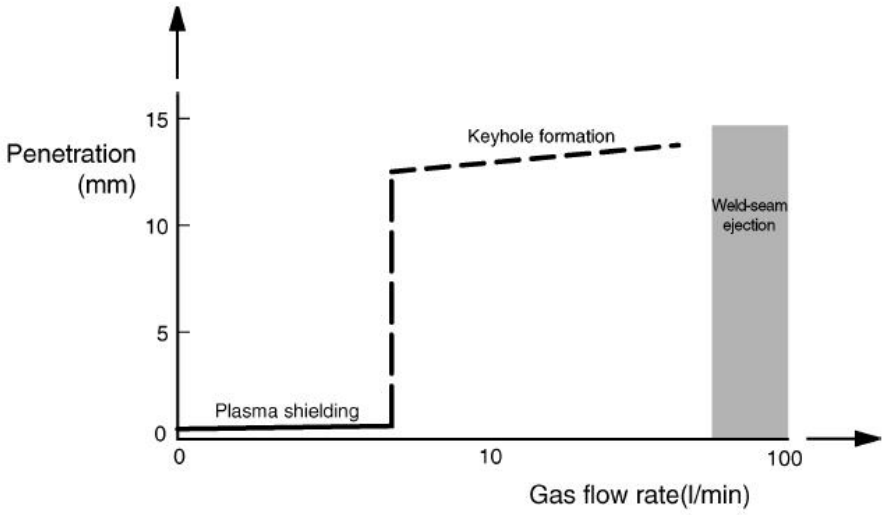

Figure 2.12. Effect of gas flow rate on penetration depth and keyhole formation.
(Steel, 10 kW, Helium, 1.2 m/min.) (Source: Beyer et al. 1988)

Focal distance (spot size): Focal distance describes a distance between laser welding head and focused laser beam position. The distance depends on the properties of optical lens. Increase or decrease of focal distance changes the laser beam diameter on the workpiece. Therefore, the spot size together with the power affect both power density and penetration depth directly. Focal position effect on penetration depth is described in Figure 2.14. Fiber lasers provide a more finely focused beam than the traditional lasers and for a constant power, penetration results are better and welding speed is 50-100% faster than Nd:YAG lasers (Popov 2006).

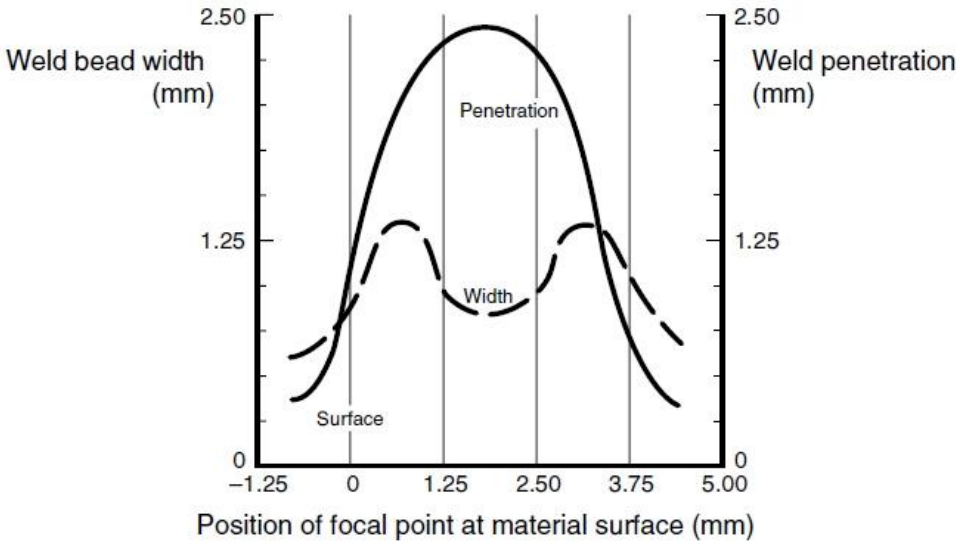

Figure 2.13. Focal position effect to penetration depth. (Steel, 1.45 kW, 1.25 m/min) (Source: Kannatey-Asibu 2009)

Joint Configuration: The common joint types are illustrated in Section 2.3.4. Pre-process sensing techniques and allowed gap between workpieces are presented above. When the gap is bigger than %10 of thinner material's thickness, most or the entire beam will pass directly through the gap and results in a defect. To overcome the small beam size problem, the beam could be defocused to increase spot size but that decreases power density and hence laser beam absorption. This may result in fluctuations in absorbed energy by workpiece. Use of fiber laser for industrial applications minimizes that fluctuation thanks to 1060 nm wavelength which is easier to absorb by metals (Steen and Mazumder 2010).

Beam Characteristics: Both pulsed and continuous wave laser modes are convenient for laser welding. For spot welding or micro welding, pulsed wave characteristics are more appropriate but for a continuous welding application when large amount of energy is needed in short time periods, a CW beam is preferred. Pulsed beams could be used for continuous welds if the pulses are overlapped but additional parameters have to be calculated such as pulse duration and pulse frequency. However, shorter pulse duration for deep penetration welding results in lower penetration. In addition, multi-mode lasers have larger spot size that needs less welding path alignment. Beam stability is another requirement for repeatability and consistency of welding quality since output variations of laser source cause variations in welding process quality (Kannatey-Asibu 2009).

As mentioned above, an experimental study to define appropriate parameters has been made for a fiber laser deep penetration welding by Püskülcü and Koçlular (2009) with a continuous wave 1kW fiber laser on butt and lap joint configurations. Critical welding parameters were given for common use material types. In experimental studies of this thesis, tests are carried out by considering these parameters. Parameter tables for butt joint and lap joint are given in Table 2.3 and Table 2.4.

Table 2.3. Laser welding parameters for butt joint configuration.
(Source: Püskülcü and Koçlular 2009)

Experiment no:	Material	Thickness of 1th m. (mm)	Thickness of 2nd m. (mm)	Laser power (watt)	Welding speed (mm/min)	Shielding gas	S. gas flow rate (l/min)	Focal distance(mm)
5	SS-304	0.5	0.5	972	9000	Argon	15	202
15	Mild Steel	0.5	0.5	1057	9000	Argon	18	204
20	Al-1050-H14	0.5	0.5	1057	9000	Argon	18	202
27	Mild Steel	1	1	632	3000	Argon	15	202
40	SS-304	1	1	1040	6000	Argon	15	204
42	Al-1050-H14	1	1	1040	4000	Argon	15	202
50	Mild Steel	1.5	1.5	1040	5000	Argon	15	204
60	SS-304	1.5	1.5	1040	5000	Argon	15	204
65	Al-1050-H14	1.5	1.5	1040	4000	Argon	15	204
69	Mild Steel	2	2	1040	4000	Argon	15	204
76	SS-304	2	2	836	2000	Argon	15	204
85	Al-1050-H14	2	2	1040	1400	Argon	15	204

Table 2.4. Laser welding parameters for lap joint configuration.
(Source: Püskülcü and Koçlular 2009)

Experiment no:	Material	Thickness of 1th m. (mm)	Thickness of 2nd m. (mm)	Laser power (watt)	Welding speed (mm/min)	Shielding gas	S. gas flow rate (l/min)	Focal distance(mm)
6	SS-304	0.5	0.5	1040	8000	Argon	15	202
12	SS-304	0.5	1	1040	5000	Argon	15	204
21	SS-304	0.5	2	1040	1500	Argon	15	202
33	SS-304	1	2	1040	800	Argon	15	202
38	SS-304	1.5	1.5	1040	1000	Argon	15	202
48	Mild Steel	0.5	0.5	1040	9000	Argon	15	202
51	Mild Steel	0.5	1	836	3000	Argon	15	204
87	Al-1050-H14	0.5	0.5	768	3000	Argon	15	204
90	Al-105-0H14	0.5	0.5	1040	7000	Argon	15	204
94	Al-105-0H14	0.5	1	1040	3000	Argon	15	204

2.6. A Review on Sensing Techniques and Conclusions

To summarize the literature survey, laser welding sensing techniques which are applied to different materials at different thicknesses are tabulated in Table 2.6 (where Table 2.5 provides the numeration details for Table 2.6). In addition to what have been presented for previous work on monitoring and control of laser welding process, other works on this subject are summarized and discussed below.

After the work of Tönshoff (2002) and Sun and Kannatey-Asibu (2002), several photodiode based techniques are integrated to obtain emitted information. Bagger (2003) placed a photodiode under the workpiece. The system achieved a full penetration closed-loop control by controlling the power. Unlike the others, Sanders (1998) used an infrared sensor to detect part misalignment and surface contamination.

Imaging of keyhole and weld pool geometry requires a CCD or a CMOS camera and fewer signal processing needs rather than monitoring and processing all sensed signals of photodiode-based techniques. A straightforward method studied with both camera and photodiode is given in the work of Kawahito and Katayama (2005). They have introduced an adaptive control to a laser spot welding. Laser source and welding

head manufacturers developed compatible systems for both photodiode and camera inspection systems. Weldwatcher (Postma et al. 2002), Fraunhofer ILT (Petereit et al. 2002) and Precitec (Kogel-Hollacher et al. 2004) companies introduced their systems in related papers.

For pre-process control of laser welding, Kessler (2003) introduced monitoring with two different methods. In this work, not only pre-process requirements to predict defects are studied but also post-process methods to detect defects are considered. Wiesemann (2004) accomplished the same type of monitoring by using different type of laser sources and described a sensor guide for pre-processing. For recognition of weld joint initial position, inadequate studies for industrial environment have been presented (Zhu et al. 2005, Kong et al. 2007, Shi et al. 2007). They introduced different image processing algorithms to define welding joint trajectory but in experimental setup, they only used high-contrast materials like aluminum or polished metal and basic path configurations, which are not common in industrial environment. Also, they conclude their search only in pixel units that needs additional calibration methods to adapt any kind of real world application. However, an intelligent method on off-line robot programming by using a CAD drawing is described to adjust virtual positions of a robot to global positions in the work of Neto and Mendes (2013). They automatically extracted motion data from a CAD drawing and made a mapping of data from virtual to real environment. To calculate kinematic errors a camera calibration survey was presented in their paper.

Table 2.5. Legend of Table 2.6.

Laser Type	**Material**	**Joint**	**Defect**	**Inspection Type**	**Sensor**
1. CO_2	8. Al-Alloy	14.Butt joint	19.Blow-out	28.Pre-Process	31.CCD, CMOS-camera
2. Nd:YAG	9. Low C-steel	15.T-Joint	20.Void	29.In-process	32.Plasma/ photodiode
3.Continous wave (CW)	10.Stainless Steel	16.Lap Joint	21.Crack		33.Thermal/ photodiode
4.Pulsed wave (PW)	11.Titanium alloy	17.Spot weld	22.Pores		34.Laser reflect/ phodiode
5.Hybrid Welding (MIG)	12.Zn - coated steel		23.Undercut		35.Acoustic /mic.
6.Fiber Laser	13. Inconel		24.Reinforcement		
			25.Root drop-out		
			26.Lack of fusion		
			27.Lack of penetration		

Table 2.6. A review for sensing techniques.

No	Author	Country	Laser System	Laser Mode	Power	Material	Thickness	Joint Type	Defect	Inspection Type	Monitoring Sensor	Control Loop
			CO_2/ Nd:YAG Fiber	CW - PW	kW		mm					
1	Bagger	DK	1	3	1,5	8	5-1,25-2-3	16	27	29	33	+
2	Sanders	US	1,2	3,4	6		5			28	33	
3	Tönshoff.	D	1, 5	3	6	9	10	15	22 27	29	31 32	
4	Sun	US	1	3	1,1-7,4	9	0,91-1,2	16	27	29	32 35	
5	Kawahito	Jpn	2	4	0,05	8	0,1-1	17	26		31 33 34	+
6	Bad'yanov	Rus	2		1,4	9	0,5	16	27	29	31 34	
7	Postma	Ned	2		2	9	0,7	14	27		32 33	+
8	Petereit	D	1, 2						27	28	31 33	
9	Kogel-Hollacher	D						14		28	31	
10	Bardin	UK	2		4-2,5	11 13		17	27	29	31 33	+
11	Gu	Can	1		1,7	9	1	14-16	27	29	35	
12	Li	UK	1		2	9	5			29	35	
13	Li	UK	1	3, 4	1,5-5	8-9-11-12	2-0,22-1,5	14-16-17	27	29	32	
14	Kessler	D	1, 2	3					19 21 26 27	28	31	+
15	Wiesmann	D	1,2							28		+

(cont. on next page)

Table 2.6. (cont.)

No	Author	Country	Laser System	Technique	Power	Material	Thickness	Joint Type	Defect	Inspection Type	Monitoring Sensor	Control Loop
			CO_2/ Nd:YAG Fiber	Cw/ Pw	kW		mm					
16	Shao	UK	1,2						19 21 27	28	31 35	
17	Ostendorf	D	2							29	32 33	
18	Park	Kor	1		6					29	34	
19	Kannatey	Ca n	1	3	5		5			28 29	31	+
20	Bertrand	F	2	3	3	9-10		14		29	33	+
21	Kaierle	D	2		3		1	14		28 29	31	
22	Jeng	Tai	1		2	9	0.5-3	14		28	31	
23	Ge	Chi				10				28	31	
24	Shen	Chi				8				28	31	
25	Shi	Chi				-				28	31	
26	Neto	Por								28	31	

With development of robotized welding, improved sensing techniques and increasing automation demands, more welding robots have been used in industry in recent years. However, they are still programmed with conventional teaching process (based on manuel position recording) which is time-consuming and inadequate for laser welding position accuracy requirements. As described in this chapter, laser welding process requires high precision for joint alignment and seam path recognition. Once welding parameters have been verified, pre-processing applications are becoming more significant. Considering gap limitations due to laser beam diameter, welding quality criteria has to be determined at the beginning of the process. However, the survey on this subject introduced that there is still a requirement to define and modify a laser welding path with high accuracy at an affordable price.

In this thesis, a vision-based seam path modification and off-line programming method are implemented to the experimental setup so that the operation could be completed in high repeatability with high accuracy. For this purpose, a vision camera and three-axes laser welding machine are used to implement the developed vision algorithm. To convert image coordinates to real world coordinates, a CAD-based correction is described in Chapter 4. An efficient calibration method is implemented in experimental setup to increase the level of measurement precision.

In experimental setup, the 1 kW continuous wave fiber laser and the manufacturing environment is provided by Lazertek Tasarım Company for tests. Next chapter includes theoretical explanations on applied subroutine method, calibration method to measure the offset between the laser spot and initial position of the weld path in mm and control architecture of the technique.

CHAPTER 3

SUBSYSTEMS

The development of robotic laser welding systems have contributed to development of vision technology and advanced image processing algorithms. The automation process of laser welding using the combination of these image processing algorithms has attracted attention of machine vision companies. Requirements of high accuracies in fixing the workpiece and joint geometry definition for laser welding process necessitates the use the vision subsystems with motion controller systems. Therefore, the pre-processing technique is presented in this chapter with the help of a process flowchart. The applied technique is composed of two subsystems; a machine vision system and a CNC system. The integrations of these systems constitute the end of this chapter.

In pre-processing measurement systems, a set of known features of the workpiece is computed. Machine vision companies provide package solutions such as size, position, orientation and contour measurement. However, laser welding calls for other types of measurements as well because of its different application field. Thus, an industrial vision system should achieve high accuracy on measurements consistently. Each application has its own characteristics and generates irregularities in measurements so tasks have to be undertaken such as what kind of information should be retrieved and how this should be translated into measurements or features extracted from image. Large amount of laser welding applications are carried out on different materials in the industrial environment. Therefore, laser spot position based measurement is implemented to solve contrast failures for feature extraction since laser pointer provides reliable and useful information for machine positioning. For more accuracy, a CAD based correction and measurement method by using laser spot position is studied in this work for a feasible system that can be applied in most applications. In this chapter, operational information and modification codes are described step by step with a flow chart of process. An overview of the whole method is illustrated in Figure 3.1.

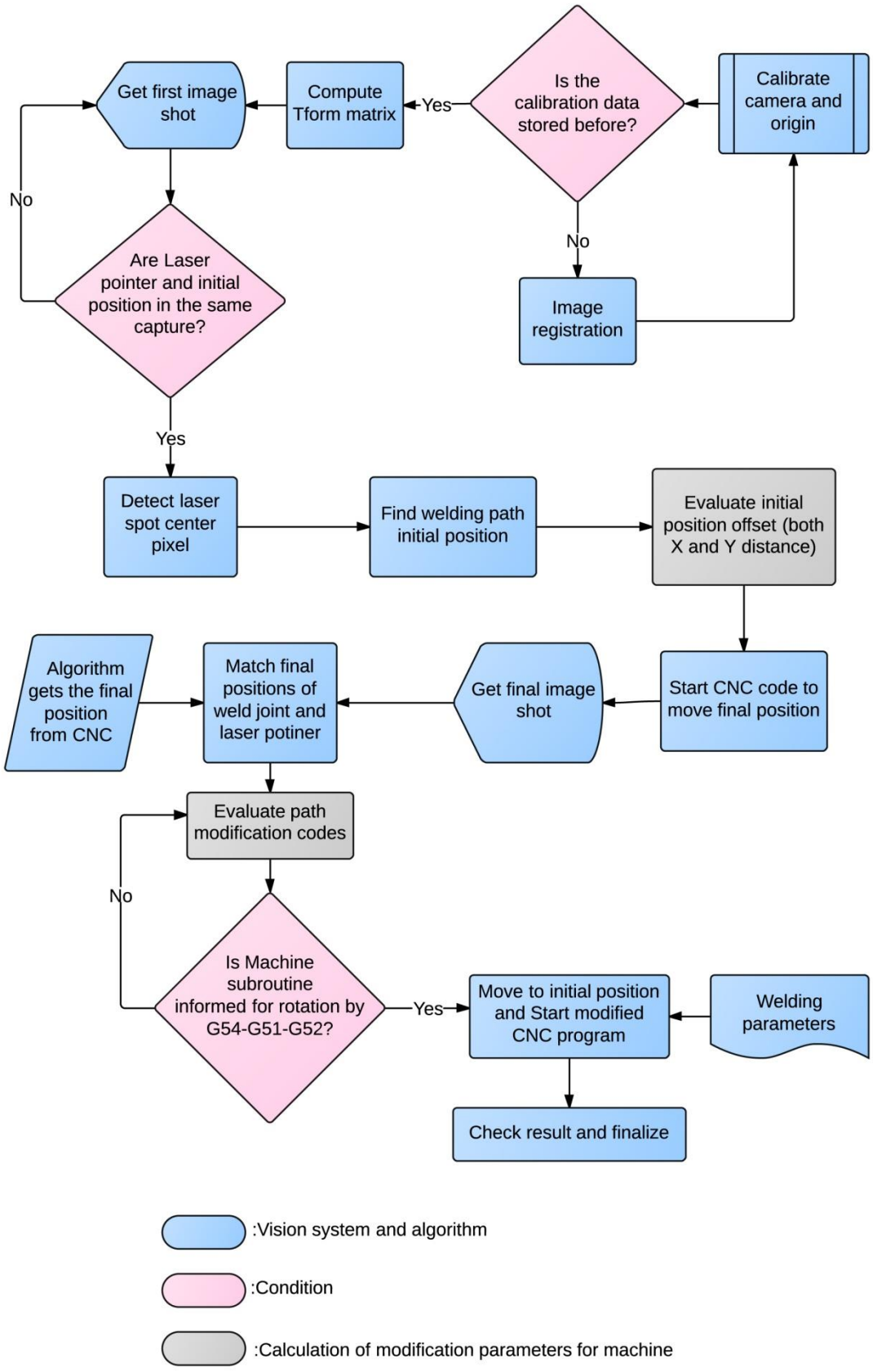

Figure 3.1. Flowchart of the process.

Calibration of machine vision system is the first step of the process which is required for projective planar measurements because vision camera is not positioned to laser welding head co-axially. Therefore, images are not taken from a planar surface. The calibration process results in a computed transformation matrix, which is used for correcting the distortions of a taken image from a projective plane. A detailed description of conversion of projective plane coordinates and correction of distortions are given in Section 3.1. Measurements are taken from the transformed image.

For final image capture, CNC program that contains the position information of motion is activated to move to the terminal position of weld joint without activating laser emission. The unmodified CNC program has to be run free for one pass to modify codes for target path. Once both initial and final images are captured, the algorithm extracts a subprogram that contains evaluated transition, rotation and scale parameters to modify the main program. The modification data can be imported and changed adaptively while the main CNC program is running. The execution of subprogram cycle is described in Section 3.2.

Another condition for initiation of the measurement is that laser pointer and initial position of welding path has to be in the same captured image. Identification of spot size position is critical for measuring both initial and final position of weld joint since the subsystem interactions depend on that position. The laser spot position and machine position relationship are presented in system integrations part in Section 3.3.

3.1. Machine Vision System

The machine vision system is one of the subsystems used in the experimental setup. The system interacts with the machine position relatively by using laser spot size center pixel. Related pixel is used to inform the machine to modify seam path. In order to validate the measurements, welding positions are obtained with the support of vision algorithm before calibration process is identified properly.

Camera calibration is an operation of calculating the intrinsic, extrinsic and lens distortion parameters of the camera. These parameters are used to remove lens distortion from an image and conduct measurements on a planar object. Performance of measurement system depends on calibration accuracy directly (Eddins et al. 2004). Therefore, calibration requirements have to be defined properly. In experiments the

camera calibration is done by using a check board grid pattern with known dimensions. The check board is used for a corner extraction feature to map existing points both in image and world coordinates. This mapping process will describe a geometric transformation which converts image points to millimeters. A typical calibration process workflow is illustrated in Figure 3.2.

Figure 3.2. Camera calibration workflow.

Preparation: A check board pattern that consists of equal squares has to be prepared in a rectangular geometry and not in square. Otherwise, the pattern does not contain two black corners along one side opposite two white corners on the other side. This criterion determines the orientation of the pattern. The longer side is assigned as x-direction. Also, the check board must be located on a flat surface for better accuracy and check board square size must be defined properly.

For stability of measurements, the camera focus should not be changed and if camera lens provides zoom variations, zoom settings must be fixed during calibration and measure process otherwise, focal length changes.

Load images: The images of check board must contain entire check board for a proper corner extraction. A blurry image or an extremely angled image will affect the accuracy of calibration.

Calibrate: To define a calibration process, a camera projection model is used, which is called as “Pinhole Camera Model” (Figure 3.3), before finding intrinsic and extrinsic parameters of the camera.

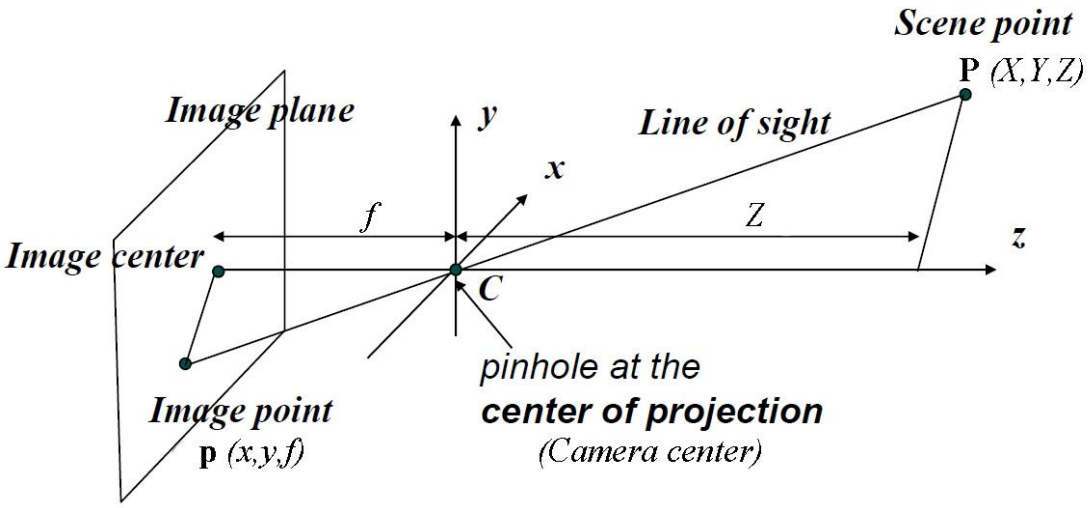

Figure 3.3. A pinhole camera model.
(Source: Fusiello 2005)

The pinhole camera model is presented to describe perspective imaging. Point "C" is the center of projection, principle point "p" is a point on image plane and the distance between image plane and camera center "f" is focal length. The point on the image plane, which corresponds to a world point "P" in the scene, is found by following the line of sight that passes through the world point and the center of projection. When center of projection "C" and image plane axis are parallel to Z axis, a view of pinhole camera on Y-Z plane is illustrated in Figure 3.4. and principle point coordinates are represented in Equation 3.1 (Banerjee 2008).

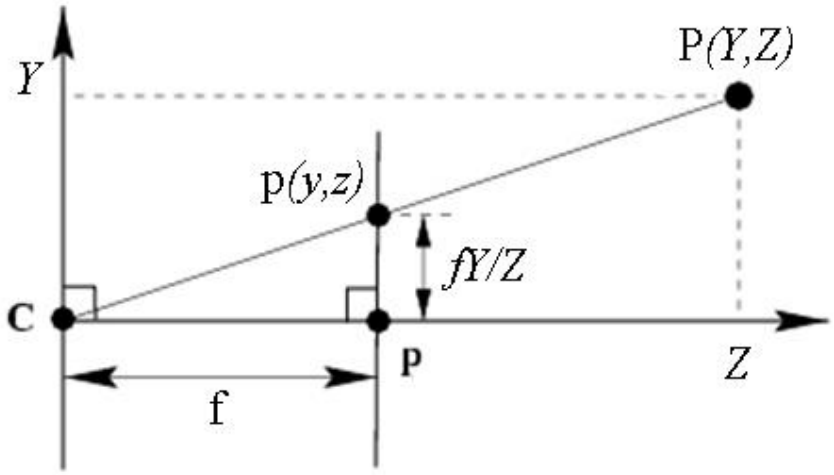

Figure 3.4. Pinhole camera model – principle point position.

If the world coordinates of P point are *(X,Y,Z)* and the image coordinates are *(x,y)*, then

$$x = \frac{fX}{Z}$$
$$y = \frac{fY}{Z} \tag{3.1}$$

Equation 3.2 can be written by using the homogeneous image plane coordinates (P_i) for point p, where *f* is focal length

$$\begin{pmatrix} x \\ y \\ 1 \end{pmatrix} \sim \begin{pmatrix} fX \\ fY \\ Z \end{pmatrix} = \begin{bmatrix} f & 0 & 0 & 0 \\ 0 & f & 0 & 0 \\ 0 & 0 & 1 & 0 \end{bmatrix} \begin{pmatrix} X \\ Y \\ Z \\ 1 \end{pmatrix} \tag{3.2}$$

If the pixels are square, the resolution will be identical in both x and y directions of the image coordinate. With the condition of parallelism of image plane and projection plane;

$$\begin{pmatrix} x \\ y \\ 1 \end{pmatrix} \sim \begin{pmatrix} fX \\ fY \\ Z \end{pmatrix} = \begin{bmatrix} f & 0 & 0 \\ 0 & f & 0 \\ 0 & 0 & 1 \end{bmatrix} \begin{bmatrix} 1 & 0 & 0 & 0 \\ 0 & 1 & 0 & 0 \\ 0 & 0 & 1 & 0 \end{bmatrix} \begin{pmatrix} X \\ Y \\ Z \\ 1 \end{pmatrix} \tag{3.3}$$

This can be expressed in form as

$$\mathbf{x} \sim \mathbf{K}[\mathbf{I}|0]\mathbf{X} \tag{3.4}$$

Where "**K**" is the intrinsic matrix that is only related to the optical properties of camera but in reality, "**K**" depends on not only focal length but also principal axis and lens distortion parameters, which is presented in Equation 3.5. In Equation 3.5, "s" is the skew distortion and (x_0 , y_0) is the image plane coordinates.

$$\mathbf{K} = \begin{bmatrix} fa & s & x_0 \\ 0 & f & y_0 \\ 0 & 0 & 1 \end{bmatrix} \tag{3.5}$$

However, calibration process problem includes also extrinsic parameters like rotation, translation which depend on where the camera is located.

If the center of projection is not positioned at (0,0,0) and the camera is oriented arbitrarily (when z axis is not perpendicular to image plane), then a rotation and translation matrix to shift camera coordinate system is to be used to define configuration as in Figure 3.3. The translation of camera to origin of *XYZ* coordinate system is given by $T(T_x,T_y,T_z)$ and the rotation applied to coincide the principal axis with *Z* axis is given by a 3x3 matrix ***R***. The extrinsic parameter matrix formed by first applying translation followed by rotation matrixes is given by the 3x4 matrix;

$$E = (R \mid RT) \quad . \tag{3.6}$$

The complete camera transformation can be provided as

$$K(R \mid RT) = (KR \mid KRT) = KR(I \mid T) \tag{3.7}$$

So world coordinates P is translated from image coordinates P_i as;

$$P = KR(I \mid T)P_i = CP_i \quad . \tag{3.8}$$

The complete calibration matrix "***C***" is a 3x4 matrix since P_i needs to be in *4D* homogeneous coordinates and P derived by CP_i will be in *3D* homogeneous coordinates. The exact 2D location of the projection on the camera plane will be obtained by dividing the first two coordinates of P by the third.

Evaluation: A projective camera model is used to make the image plane parallel to the camera center plane so that pixel coordinates can be converted into world coordinates by a transformation matrix. The measurements that are implemented in pre-processing method depend on this conversion from projective plane to planar plane as illustrated in Figure 3.5.

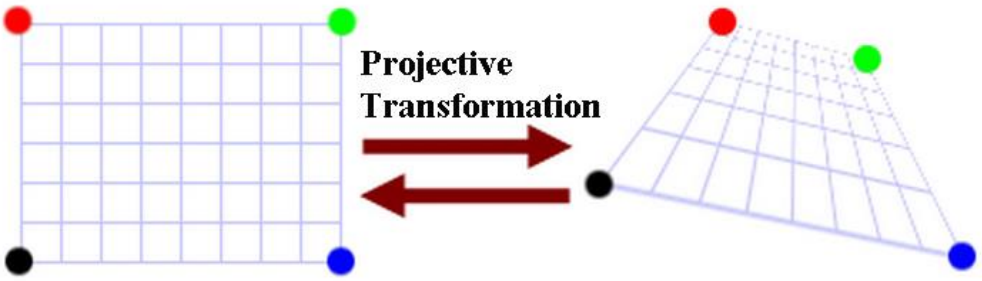

Figure 3.5. Projective transformation.

In the applied vision algorithm, taken images from vision camera are modified with a correction of distortion algorithm that transforms a 3D scene point into a 2D image point and general projective mapping from 3D to 2D plane can be demonstrated as;

$$\begin{pmatrix} x_1 \\ x_2 \\ x_3 \end{pmatrix} = \begin{bmatrix} T_{11} & T_{12} & T_{13} & T_{14} \\ T_{21} & T_{22} & T_{23} & T_{24} \\ T_{31} & T_{32} & T_{33} & T_{34} \end{bmatrix} \begin{pmatrix} X_1 \\ X_2 \\ X_3 \\ X_4 \end{pmatrix} \tag{3.9}$$

Where $(x_1, x_2, x_3)^T$ and $(X_1, X_2, X_3, X_4)^T$ are homogeneous coordinates related to *x* and *X* by

$$(x, y) = (x_1 / x_3, x_2 / x_3) \tag{3.10}$$

$$(X, Y, Z) = (X_1 / X_4, X_2 / X_4, X_3 / X_4) \tag{3.11}$$

After an image is transformed by a projective mapping, undistorted images are used for calculation. Suppose that (w,z) and (x,y) are undistorted two spatial coordinate systems, one is image space and other is world space respectively. A geometric coordinate transformation can be defined as

$$(x,y)=T[(w,z)] \tag{3.12}$$

Where **T** has an inverse that maps world space to image space by

$$(w,z)=T^{1}[(x,y)] \tag{3.13}$$

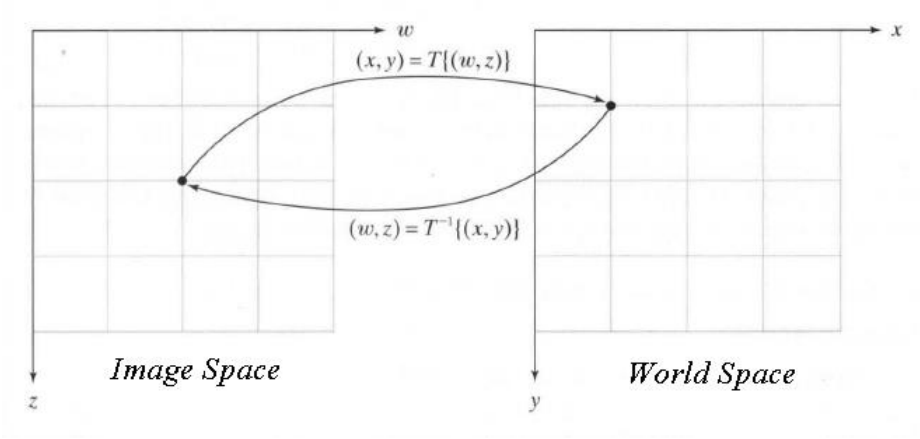

Figure 3.6. Space transformation is used for measurements.

The transformation matrix is used in space transformation of a point as shown in Figure 3.6. During the measurements, the evaluated transformation matrix provides a conversion from laser pointer position to machine position or inverse operation in vision algorithm.

Improve: High pixel-error images are removed during calibration to improve result. More images provide better accuracy. Furthermore, some camera sensors contain imperfections, which cause x and y axes to not be perpendicular that results from pixels not being rectangular. This defect is removed by evaluating skew distortion parameter s in the calibration matrix.

Export: Estimated calibration parameters are stored for future measurements.

3.2. CNC System

CNC system contains both motion control and microprocessor-based logic subsystems. The logic system consists of an industrial PC, which process CNC files line by line to generate commands for subsystems and run required PLC cases under a powerful microprocessor. While interacting with the vision system, subroutine processing is used for an effective communication during pre-processing operation.

Subroutine process is a machine pose adjustment process when a main CNC program needs to be supported by other subprograms. “Subroutine call” causes the line of coded subroutine to be processed as next NC block (CNC file that contains position or external function data) as illustrated in Figure 3.7. The NC block can be processed

for different aims such as seam line rotation, seam line position, shift of origin, repetition number of cycle or feed override. The advantage of subroutine processing is that while the main program is processing, parameter changes are implemented to subroutine NC block lines adaptively or offline.

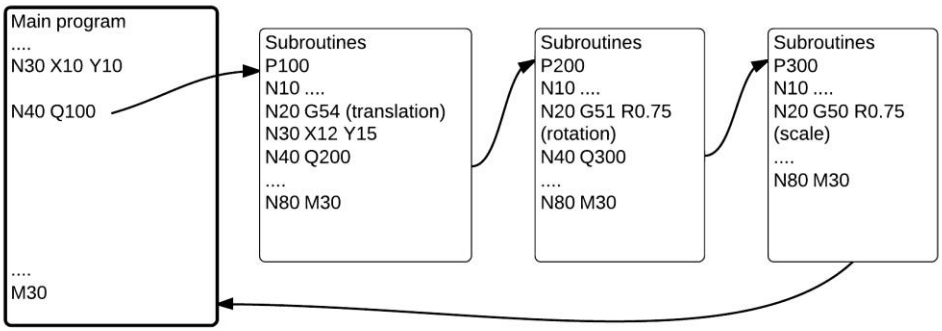

Figure 3.7. Subroutine processing.

The visual system communicates with machine CNC database by using these subroutines. Modification parameters are exported to subroutines by vision algorithm, which also analyze CNC program to import welding initial and final points, and make a relationship between machine coordinates and visual welding path coordinates.

3.3. System Integrations

Both subsystems are supported with a vision algorithm, which is necessary for communication and required control point determination of workpiece joint path with respect to laser spot position on image plane. The visual control algorithm evaluates three significant points for interaction which are enumerated in Figure 3.8.

1. Laser spot position extraction,
2. Find initial point of welding with respect to machine position,
3. Match final positions which are extracted both from CAD data and image data.

(1) Laser spot position is extracted by a circle detection method. The algorithm uses an RGB image to separate them to main colors. Red color laser spot is detected by

using red layer of image and ROI (region of interest) based image processing method. After selecting ROI, the image, which includes both laser spot and initial position of welding path, is converted to a binary image to run circle detection algorithm. Laser spot center point is the critical inspection problem that is used in algorithm to evaluate measurements both in machine and image coordinates. Therefore, the binary image is processed with a circle inspection algorithm that searches the image map for a pre-defined shape. However, the laser spot cannot be defined as a circle due to reflection of laser beam with respect to different surface quality of materials. To overcome such problem, a region-based laser spot center detection algorithm is used. Once the laser spot center point is detected, the point can be used for future measurements for equal thickness materials because it defines the constant pixel on the captured image if the camera is fixed.

(2) Initial point that was exported from CNC data is used for correlation with the laser spot center position. Initially, distortions of captured image are corrected with projective transformation matrix. Once the transformation is applied to the image, measurements are carried out by using control point selection screen. The initial position of welding path can be selected manually with improved selection tool of the algorithm. The related point can be detected by using a featured extraction algorithm automatically. However, without an external light source, the extraction parameters are not constant so automatically feature extraction algorithms for circle detection cannot be run under unstable light condition. The selection process of initial point of welding results in an initial shift for the beginning of the motion.

(3) Final position match is provided by using both extracted final point of CNC data and image measurements. Pre-defined laser spot pixel is used again to calculate machine position in the image. After final position of welding path is defined from image by using control point selection tool, the pixel distance between laser spot center and final position of workpiece joint is converted to world units (millimeter) by using the transformation matrix. The points that are calculated in steps 2 and 3 are used to estimate rotation and scale with respect to initial position of the desired welding path. At the end of the vision algorithm, a subprogram, which contains initial transition (with the parameter of G54), rotation (with the parameter of G51) and scale (with the parameter of G50) information, creates a file to be saved in destination folder of the CNC program. The implementation of the algorithm is explained in the next chapter on the experimental test setup.

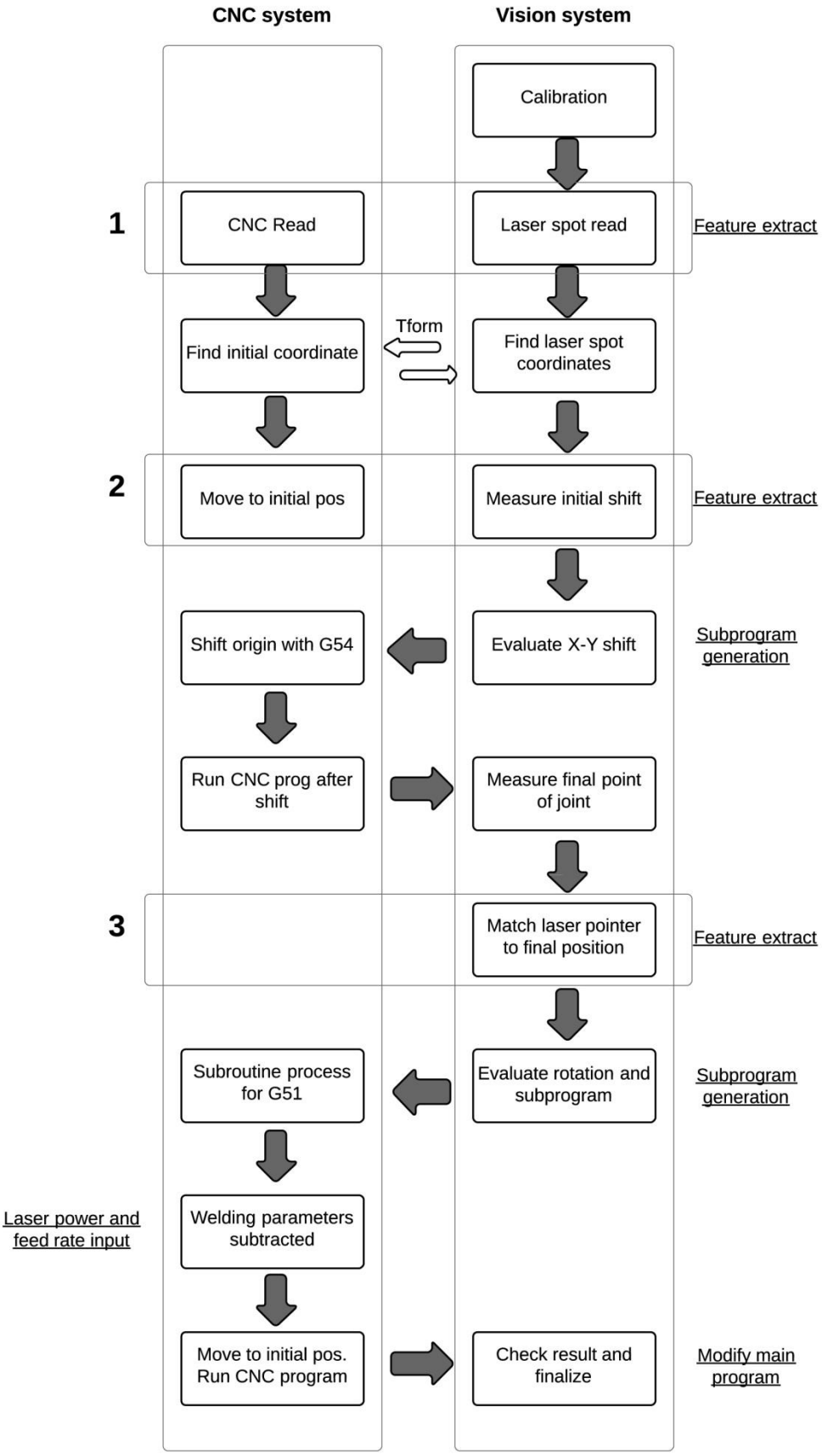

Figure 3.8. Subsystem interactions.

CHAPTER 4

EXPERIMENTAL TEST SETUP

The experiments are carried out in the Lazertek Tasarım Company with company's hardware and software in IZTECH Robotics Laboratory (IRL) that are listed in Table 4.1.

Table 4.1. Hardware and software list.

Hardware (LAZERTEK)	Software (IZTECH & LAZERTEK)
Industrial PC (Power Automation)	MATLAB© 2013b (Computer Vision Toolbox) (IZTECH)
Vision camera (Imaging Source)	DeskCNC (LAZERTEK)
Fiber laser source (IPG)	
Welding Head (Precitec)	

Vision algorithm is implemented in Matlab environment with computer vision toolbox add-on. The test procedure is carried out on a 3-axes CNC machine supported by an industrial PC where CNC codes are processed line by line. A CAD based CNC conversion is provided by DeskCNC software with predefined post-processor support. The post-processor setup tool is represented in APPENDIX A. A successful implementation of the technique is accomplished with the other main units being laser source unit combined with optical head, vision camera and CNC machine. All these units are described separately in Section 4.1.

In Section 4.2., the combination of main subsystems is presented along with the implementation of the vision algorithm. The effective use of the vision algorithm with the CNC system and the communication of subsystems are described step by step on a sample visual representation of the welding scenario. In addition, the export file to be used in subprogram routine is demonstrated by describing how modification codes are generated.

4.1.Test Setup

The experimental test setup is composed of software and hardware listed above. The hardware systems vary with the process aims. All the hardware components are chosen to be compatible products of prominent laser technology companies. An industrial PC from Power Automation provides a laser source control package with a powerful machine parameter support, which is explained in detail in APPENDIX B. Furthermore, a user friendly interface for laser power control is used that is provided by the same company.

During the tests, the working environment consists of a machine interface, a camera, which is mounted to laser welding head for monitoring welding zone, a three-axes CNC machine and an external computer to run vision algorithm. A capture of the calibration tests is illustrated in Figure 4.1. along with a calibration pattern that is located in machine workspace and inside of camera's region of interest.

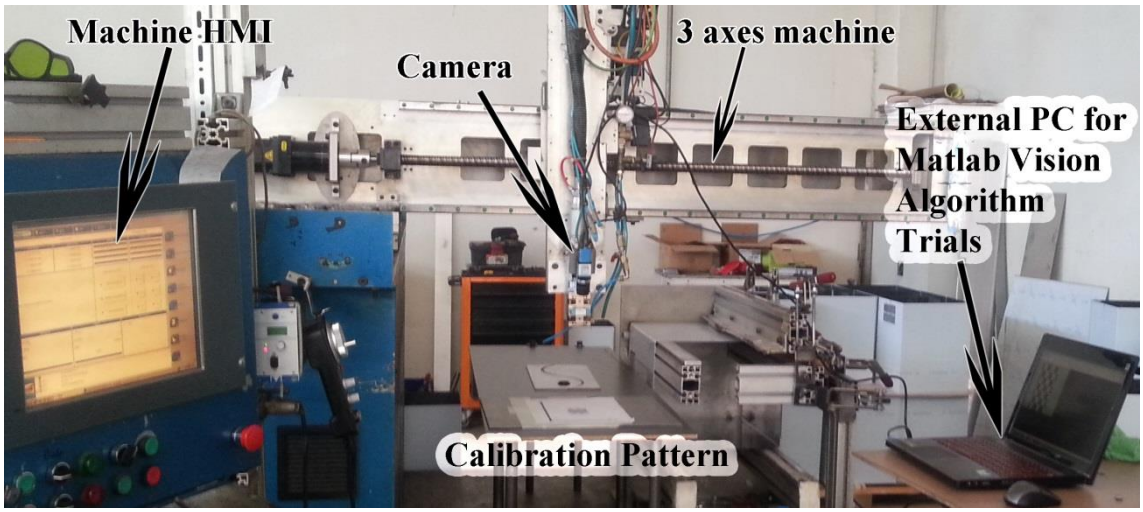

Figure 4.1. Experimental test setup.

In the implementation of the vision algorithm, the developed interface and control point selection tool helps for measurements of laser spot center point and welding path initial and final positions. Thanks to the laser pointer center detection algorithm, machine position is fed into the image plane as a virtual validation feedback. The algorithm logic was described in Chapter 3.

Laser system contains a power source and an optical laser head, which communicate with each other during the emission process. Laser source transmits signals in real-time from laser head to protect optical system in an emergency condition.

In this thesis work, bilateral communication of hardware and software subsystems is implemented by considering laser welding process requirements. For positional accuracy, a CAD based modification technique and its implementation on test samples are described at the end of this chapter.

4.1.1. Laser Source and Welding Head

Laser Source: During the tests, a 1kW continuous wave laser power supply of IPG Company is used. The body of ytterbium fiber laser unit is illustrated in Figure 4.1. A communication interface unit is used to check the related source parameters while integrating the systems and test-mode allows the creation of different pulse configuration to provide emission of laser beam for different experimental environment. The laser beam is contained within optical fiber and delivered through an armored flexible cable. Technical details of the laser source unit are represented in Table 4.2.

Figure 4.2. Ytterbium Laser System 1 kW.
(Source: IPG)

Table 4.2. Technical details of 1 kW Ytterbium laser source of IPG company. (Source: IPG)

Description	Compact kW fiber laser system
Standard Features	Randomly polarized, 1070-1080 nm emission wavelength, ytterbium doped, red aiming diode
Available Operating Modes	CW, PW
Available Output Power	500 Watts – 2 kW
Feed Fiber Diameter	50, 100, 200 or 300 μm
Wall-plug efficiency	>30%
Air conditioner	Standard
Interface	Standard: LaserNet, Digital I/O, Analog Control
Laser Cabinet Style/ Dimensions	558x790x815 mm
Upgradeable	Yes, maximum 2kW

Welding head: Welding head can be used for all fiber guided solid state lasers of 1 kw to 20 kw power range. Modular structure makes it adjustable for different laser welding applications such as process monitoring, seam tracking, beam guidance, hybrid welding systems. The basic structure of Precitec YW52 Laser Welding Head is illustrated in Figure 4.2.

The first task of an optical welding head is steering the laser beam with a collimator lens. Thus, scattered laser light that reaches the welding head will have a smooth spectrum. The optical lens focuses the rectified laser beam to a single point. A protective glass is positioned at the end of the head to prevent optical tools during welding.

The focal length, which is illustrated in Table 4.3, defines directly the focusing distance between welding head and workpiece that changes depending on the application.

Figure 4.3. Welding head. (Precitec YW52 basic mode)
(Source: Precitec)

Table 4.3 Technical details of Precitec laser welding head.
(Source: Precitec)

Max laser power	20kW
Collimation focal length	100mm-125mm-150mm-200mm
Focal lengths	150 to 1000mm
Weight	3 kg with optics
Dimensions	74x74mm (edge measurement)

4.1.2. Vision Camera

The Imaging Source vision color camera is used for implementation of vision algorithm. Sensitive vision sensor with high sensitivity is required for unilluminated environment measurements. For better accuracy, the camera is mounted on laser head and calibrated through developed calibration software implemented through Matlab. A 12mm lens is used with the vision camera to monitor the workpiece and region of interest as illustrated in Figure 4.3. Technical detail of vision camera is represented in Table 4.4.

Figure 4.4. Vision camera. (Imaging Source_DFK 23U618)
(Source: Imaging Source)

Table 4.4. Technical details of Imaging Source vision camera.
(Source: Imaging Source)

Video formats @ frame rate	640 x 480 (0.3 MP), RGB32/Y800/Y16 @ 120, 90, 60, 30, 15, 7.5, 3.75 FPS
Dynamic range	8 bit
IR cut filter	Yes
Sensor specification	Sony ICX618AQA
Shutter	Global
Format	¼”
Resolution	640x480 pixel
Pixel size	5.6 µm
Lens mount	C/CS
Supply voltage	12 VDC
Gain	0 dB to 36 dB
White balance	-2 dB to 6 dB
Temperature (operation)	-5 °C to 45 °C
Dimensions	H: 29mm, W: 29mm, L:43 mm

4.1.3. CNC Machine

The CNC machine contains an industrial PC equipped with a high speed microprocessor for bilateral communication of subsystems. The extracted welding path points from vision algorithm are obtained adaptively to modify the existing main program. Before initiating the welding job, laser safety procedures and vision evaluation results are processed on an open source PLC, where other emergency cases (e.g. with respect to safe laser emission process before the machine begins to move) are processed at the same time.

The vision software, operational interface and PLC run on Windows XP embedded operating system which is developed for industrial applications.

Whole operational interface can be controlled from the same interface. For motion control, a machine parameter panel is used to optimize motion dynamics. Analogue signal module (PAMIO) is used to process analogue laser power signal along with the other signals such as shielding gas inlet valve.

With the advantage of multi-signal processing of PLC and high speed microprocessor, other subsystems can perform under the same CNC system. Laser source unit signals, servo driver interactions, emergency condition cases can be processed on the same CNC system as illustrated in Figure 4.4. During the laser welding process, the operational interface helps the operator to control welding parameters and to check the laser unit signals from PLC signal interface. The vision algorithm works independent of the system interface. However, if necessary, the shifted zero points of the machine as a result of measurements can be checked from cycle parameters interface for validation.

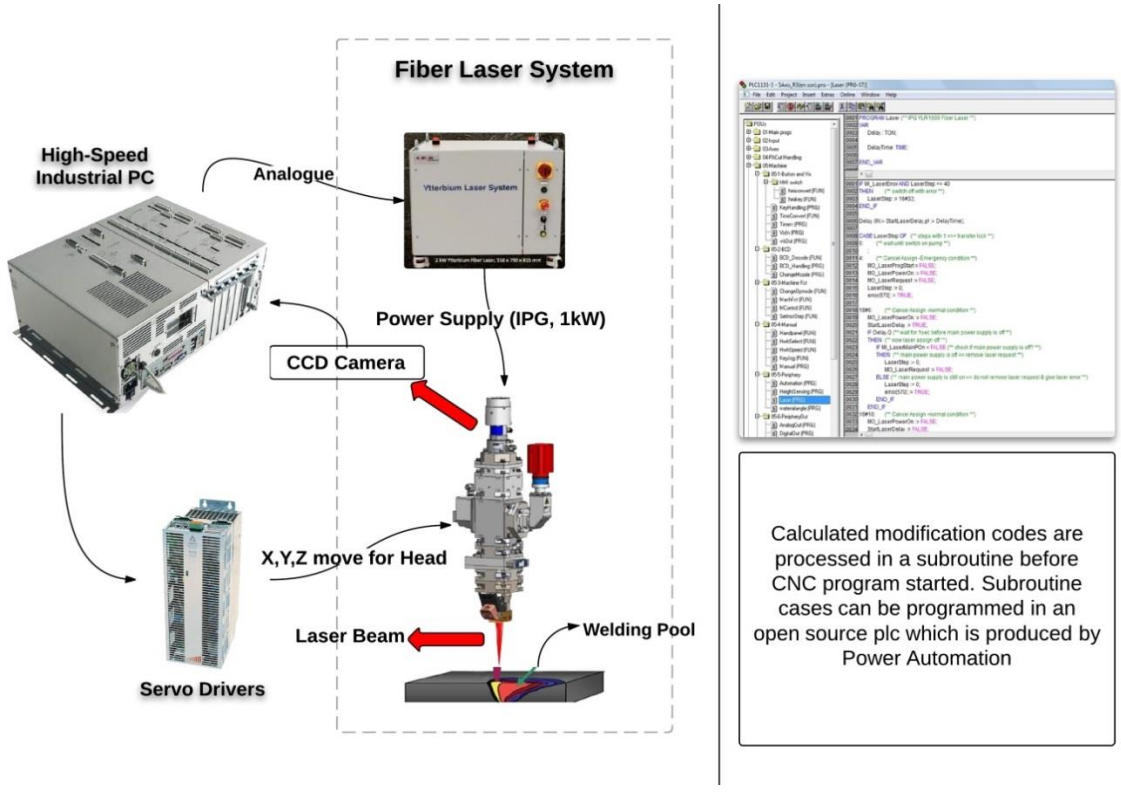

Figure 4.5. Operational subsystems run under the same industrial PC.
(Source: Power Automation)

4.2. Implementation of Control

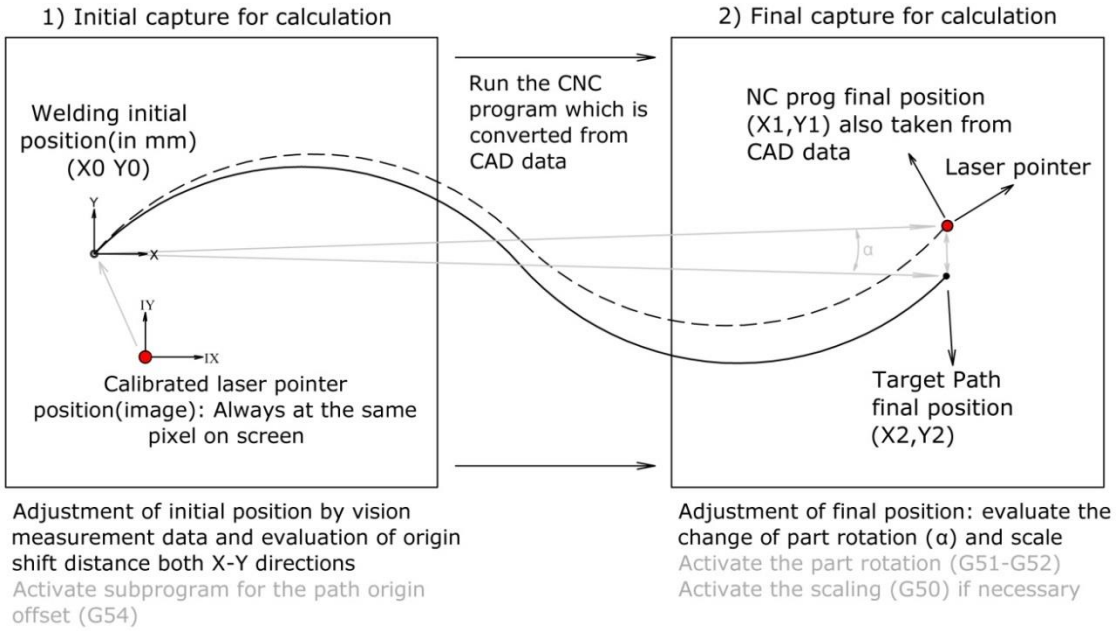

Figure 4.6. Implementation of the proposed technique.

Implementation of the technique for preprocessing of laser welding is carried out with other subsystems, which were described in Chapter 3. To use vision algorithm and generate modification codes, a CAD data of seam line is required for initial calculation since laser pointer can be used as a positioning marker to define the machine's exact position. For an initial condition, laser pointer and initial position of welding path must be in the same captured photograph; this is the only necessity for calculations which is demonstrated in Figure 4.5. The vision algorithm extracts center point of laser spot for initial calculation. To minimize detection errors of laser pointer during center point detection section, the acquired image is converted into a binary image to implement developed laser spot center detection algorithm, which was explained in Section 3.3. The shift distance calculations for initial position of target path depend on laser pointer center position to define distance in both X and Y directions (X0,Y0). The extracted pixel is used also for final capture to calculate last transition of path since the laser pointer center is always on the same pixel of captured image. A demonstration of detected circle is presented in Figure 4.6. Borders of the analyzed image signify the resolution of the captured image (640x480). Furthermore, the red circle on the image

proves the higher light intensity of red reflection zone. Center of this zone was described as laser spot center pixel during experimental tests.

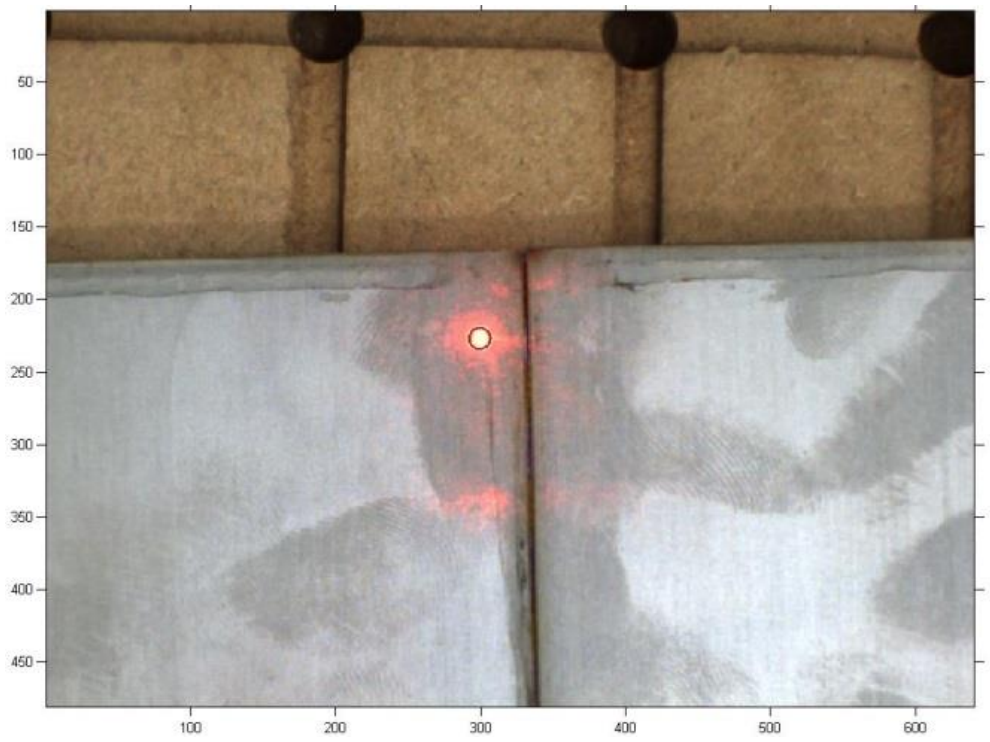

Figure 4.7. Laser spot center extraction.

To convert the pixel values into world units (millimeters), a calibration process for mapping operation of image is applied on the captured image. The details of calibration process were presented in Section 3.1. Calculation of extrinsic parameters helps to define projective position of image plane with respect to the camera position. A visualization of calibration pattern is shown in Figure 4.7. In this figure, the exact orientations of the calibration patterns are illustrated with respect to the camera position. The distance from work plane to camera is noted on Z axis in millimeters. As it can be observed, the camera is positioned around 330-360 millimeters from the checkerboards.

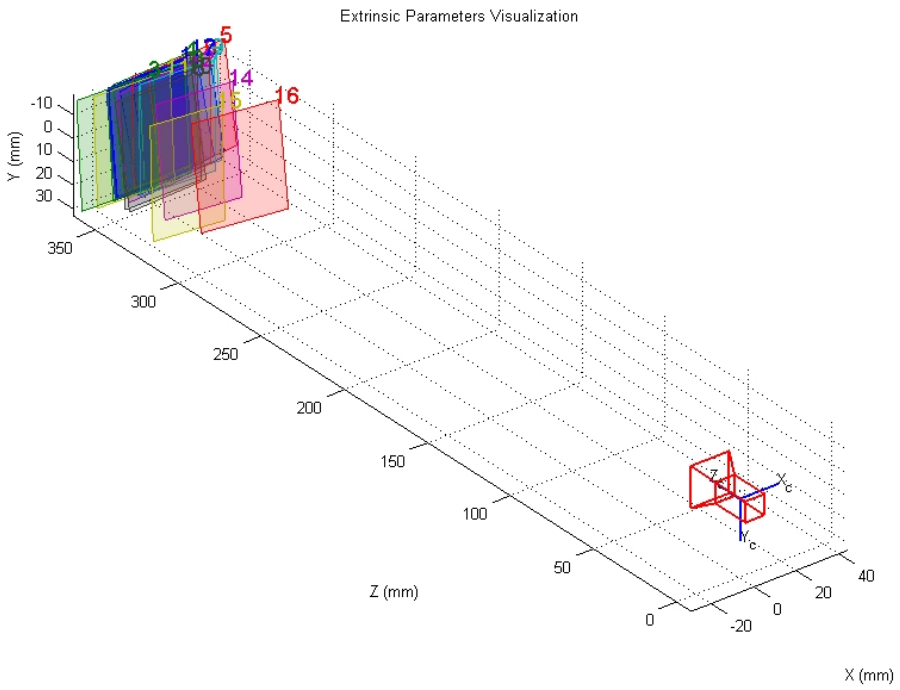

Figure 4.8. Extrinsic parameters visualization of calibration patterns.

After extracting of camera parameters, distortions of initial and final acquired images are corrected for measurements. However, to get final position of welding path, the CAD data converted by DeskCNC software (DeskCNC 2014) has to be run under test mode without activating laser emission. Once the machine reaches final position of unmodified path (X1,Y1), vision algorithm obtains target path final position (X2,Y2) to calculate shift again in both X-Y directions by analyzing exact pixel of laser pointer on the final image. These X-Y offset values are used for rotation evaluations by using a set of trigonometric functions to modify welding path at the end of the technique. After distortion correction process of both initial and final images, control point selection tool provided by Matlab is used to select the related welding path positions. The advantage of the tool is that variable ROI selection does not affect the pixel position on the image. The implementation of control point selection is illustrated in Figure 4.8. In Figure 4.8, the upper images are created within the adjusted ROI by a rectangular illustrator from the bottom images. They indicate the selected initial and final points on the target path.

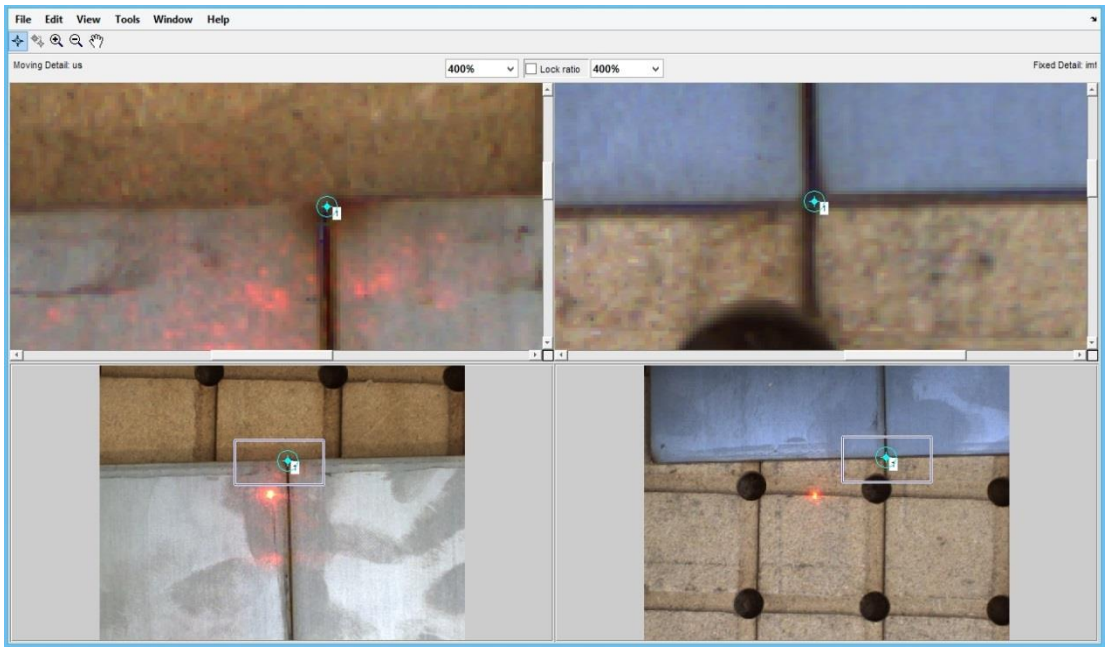

Figure 4.9. Control point selection of welding path.

Within the vision algorithm, the extracted shifts for initial and final position of joint path of workpieces result in initial shift, rotation and scale data. This information is saved as a CNC subprogram (file) under the CNC program destination folder so that operational modification is made without requiring any change on the main CNC program. The extraction of subprogram contains a series of data to set CNC cycle parameters for initial shift. In the CNC parameters, G54 code is assigned for zero point shift of the machine and G51 and G50 are assigned for rotation and scale exchange respectively. A sample extracted subprogram file is shown below:

```
%
N10 (: parameter exchange)
*N20 G54 X=-8549.1153 (: to set CNC cycle parameters)
*N30 G54 Y=15482.09 (: to set CNC cycle parameters)
N35 G00 X-8.54 Y15.43 (: go to shifted position)
N30 G54 (: activate shifted position as zero point)
N40 G51 R2.157 (: rotate main program in degree)
N50 G50 R0.998 (: scale main program)
N40 M02 (: return to main program back and implement parameters)
```

As a result of the created file, CNC machine zero points are shifted to the calculated position. Main CNC program is activated from that shifted position and modified by adjusted rotation and scale values to follow target seam line. Therefore, accuracy of the measurements influences matching performance between CAD-based data and the target path. To evaluate measurement accuracy and system performance on both X-Y axes, tests are carried out with the experimental setup. Together with the test results, the details of test criteria and test medium are presented in next Chapter.

CHAPTER 5

TEST RESULTS

Tests are carried out to assess the performance of the monitoring and control technique presented in this thesis through evaluating the accuracy of the measurements by comparing the measured and computed offset values that exported from the vision algorithm.

The obtained X-Y offset values are used to calculate deviations between reference value that is acquired from CNC machine encoders and measured value. The tests are conducted on line and curve paths for mild steel and stainless steel materials to perform another comparison for accuracy of laser pointer center point detection algorithm since threshold of images change by material and lighting condition.

During tests, Matlab version 2013b, Imaging Source DFK 23U618 vision camera and CNC machine powered by PA 8000 LW are used.

5.1. Test Parameters

The vision camera is used with resolution of 640x480 and positioned to 350 millimeter away from workpiece to monitor a 45x45 millimeter square region during the measurements. To express the system accomplishment, the effective diameter of laser spot is calculated by using the calibration value evaluated from the millimeter value for one pixel of the image. For this process, a pre-calibrated measurement tool (calliper) is used as illustrated in Figure 5.1. In the figure, the first frame shows that one pixel is equal to 0.1411 millimeter. Second frame indicates that laser spot diameter is equal to 0.9117 millimeter. However, during the tests, reliable laser spot diameter, where the density of the laser spot is relatively high, is provided by the laser source unit producing company and selected as 0.6 millimeters (600 micron). Therefore, 0.3 millimeter deviation is accepted in confidence interval.

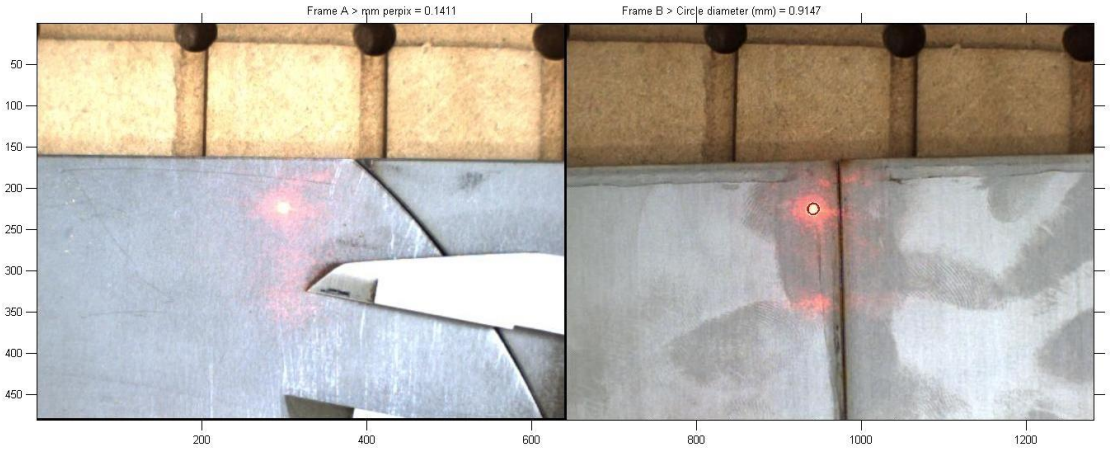

Figure 5.1. Laser spot diameter calibration.

To validate the measurements during tests, actual offset distance is obtained from CNC machine encoders to be used to calculate deviation of calculated offset distance by vision algorithm. For the accuracy of the system, the measured results through vision system are compared with machine coordinates acquired from encoder data. As a result of this, accuracy is calculated by evaluating the frequency of error occurrence. The result of accuracy test is given in the next section.

Tests are conducted for each mild steel and stainless steel plates for 30 times on line path and curve path. Welding parameters for both mild steel and stainless steel materials on butt joint configuration are taken from Table 2.3.

5.2. Line Path Modification Tests

For the line welding path experiments, 400 millimeters length plates with the butt joint configuration are positioned to machine workspace randomly. The initial and final position offset with respect to laser spot center is compared for both X and Y axes of the image and machine coordinates. The deviations after initial and final position selection of welding path on mild steel plate are illustrated in Figure 5.2 and Figure 5.3 respectively. For line path experiments on mild steel plates, 60 trials were completed for welding paths.

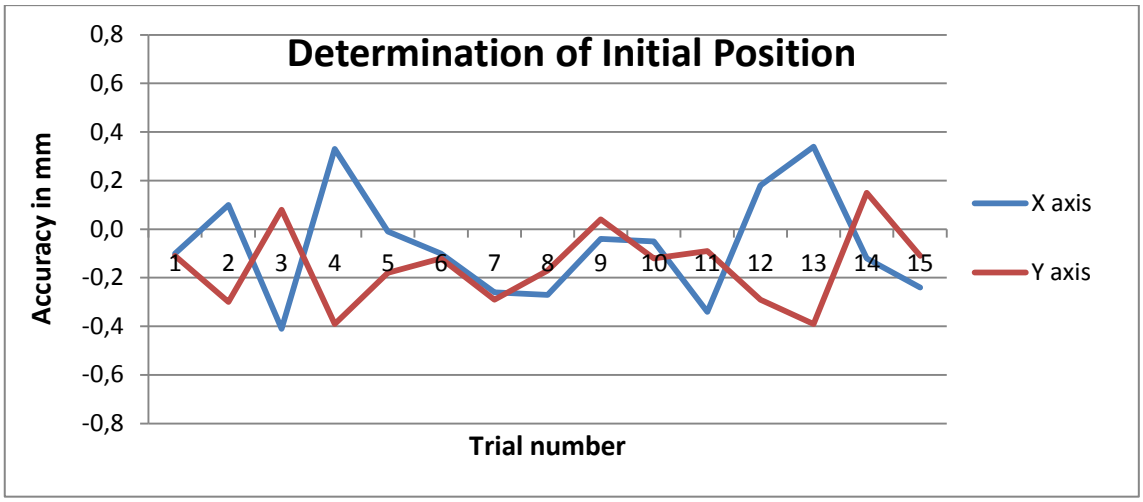

Figure 5.2. Mild steel - Line path – Initial position determination accuracy for X-Y directions.

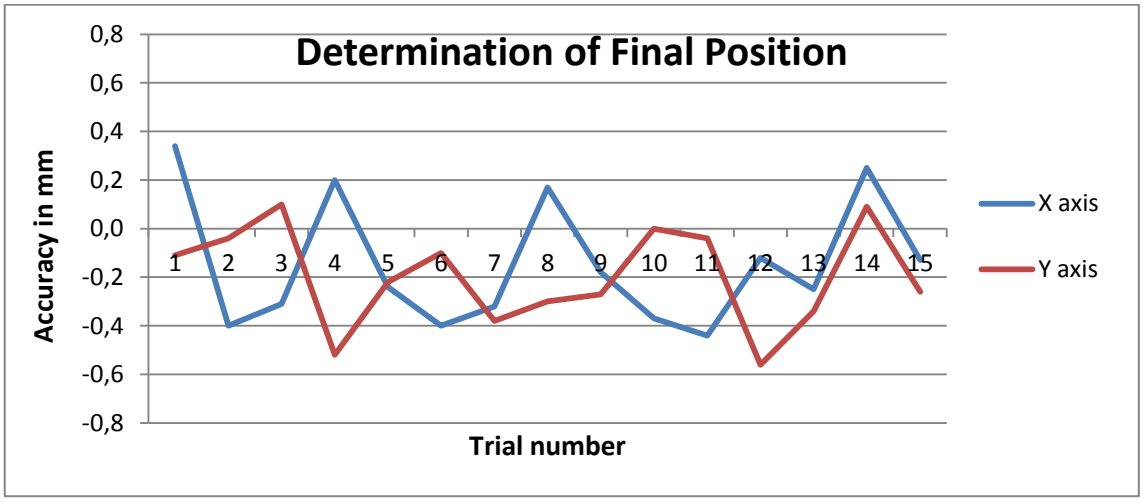

Figure 5.3. Mild steel - Line path – Final position determination accuracy for X-Y directions.

The number of measurements is reconfigured indicating acceptable deviations with respect to laser spot size in Figure 5.4. The allowed deviation on frequency distribution is given with the green bars. As it can be observed, 52 estimates (%86,66) were correct from 60 selections within 0,3 millimeters deviation.

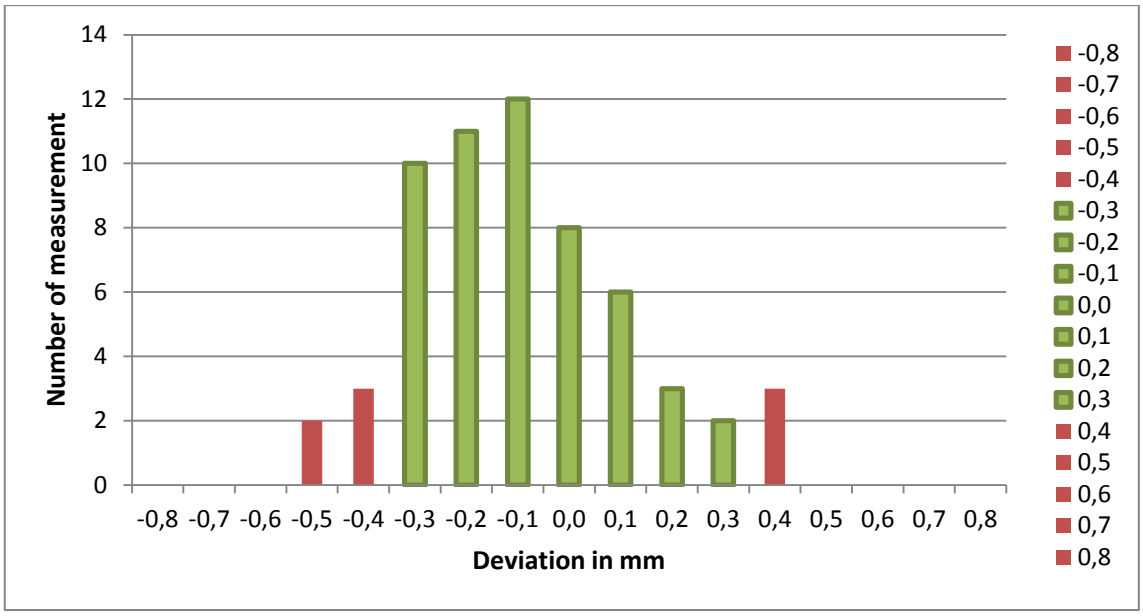

Figure 5.4. Distribution of the measurement errors for Mild steel - Line path experiments.

The X-Y offset deviations on stainless steel plate are presented in Figure 5.5. and Figure 5.6 for initial and final position determination, respectively.

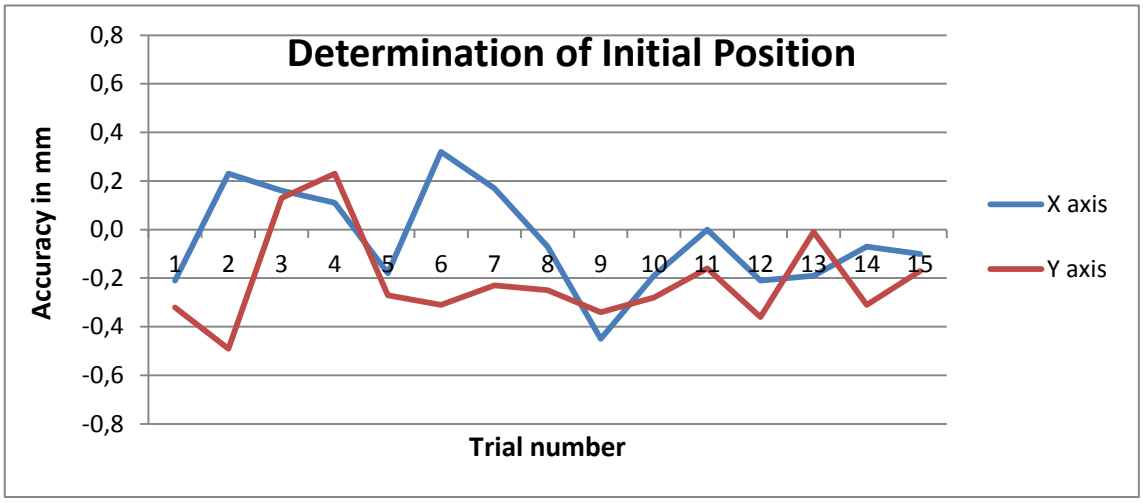

Figure 5.5. Stainless steel - Line path – Initial position determination accuracy for X-Y directions.

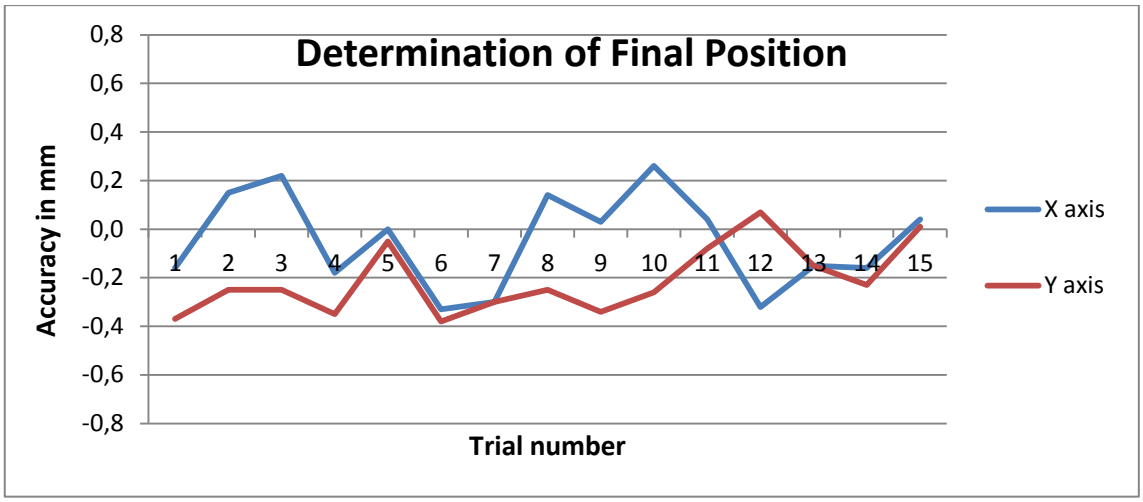

Figure 5.6. Stainless steel - Line path – Final position determination accuracy for X-Y directions.

Distribution of the errors in determination of initial and final points for stainless steel is illustrated in Figure 5.7. As a result, 57 estimates (%95) were within the acceptable range from 60 selections, which is 0,3 millimeters deviation.

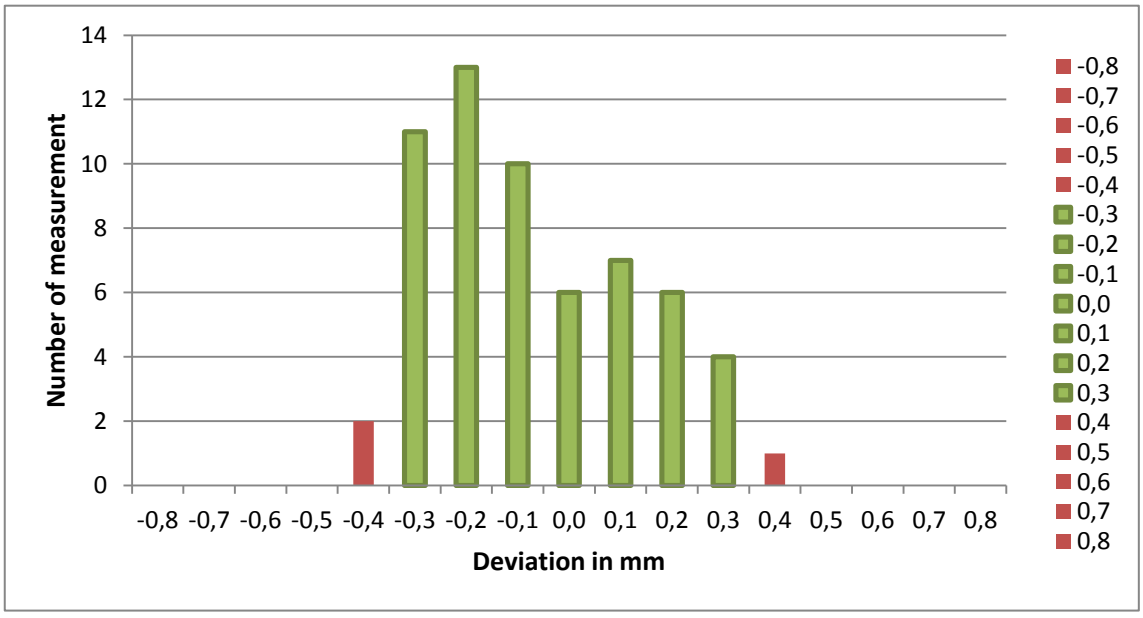

Figure 5.7. Distribution of the measurement errors for Stainless steel - Line path experiments

5.3. Curved Path Modification Tests

The tests on curved path with butt joint configuration are implemented on 400 millimeters length plates and workpieces are positioned to machine workspace randomly. The initial and final position offset with respect to laser spot center is compared for both X and Y axes of the image and machine coordinates. The deviations of position determination on mild steel and stainless steel materials are presented in Figures 5.8 and 5.9, respectively. For each mild steel and stainless steel experiment, initial and final position determinations were completed with 60 trials.

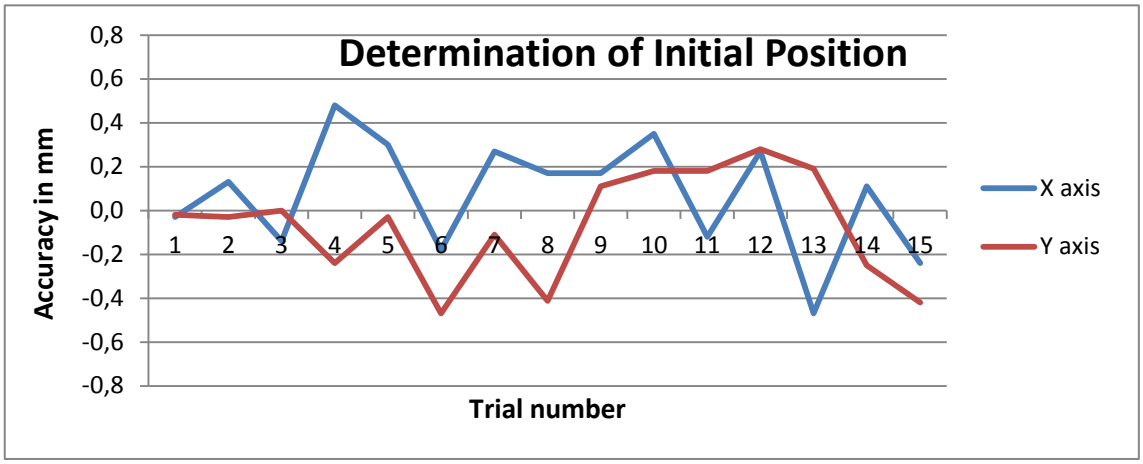

Figure 5.8. Mild steel - Curved path – Initial position determination accuracy for X-Y directions.

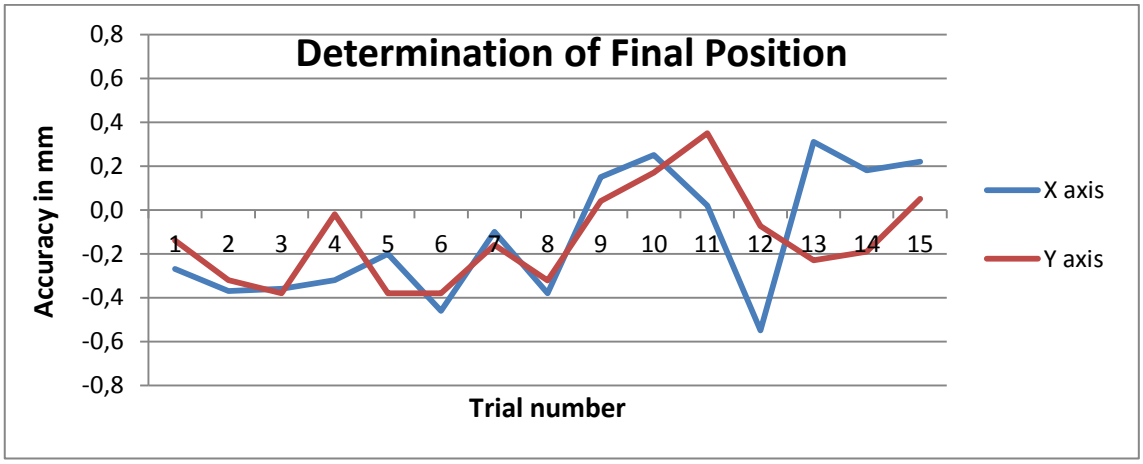

Figure 5.9. Mild steel - Curved path – Final position determination accuracy for X-Y directions.

Distribution of the errors in determination of initial and final points on curved path mild steel is shown in Figure 5.10. Regarding acceptable deviation on determination of positions, 50 position determinations (%83,33) were within the acceptable range while the remaining 10 trials were out of allowed range.

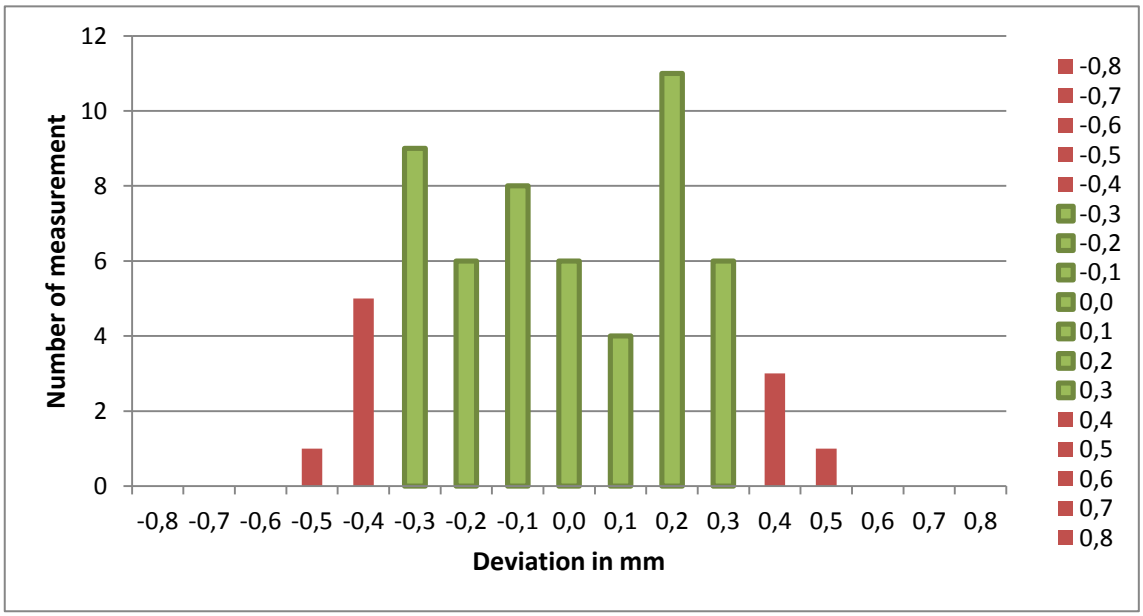

Figure 5.10. Distribution of the measurement errors for Mild steel - Curved path experiments.

The initial and final position determination of curved path tests, which are implemented on stainless steel plates, are illustrated in Figures 5.11 and 5.12 for both X-Y direction deviations, respectively.

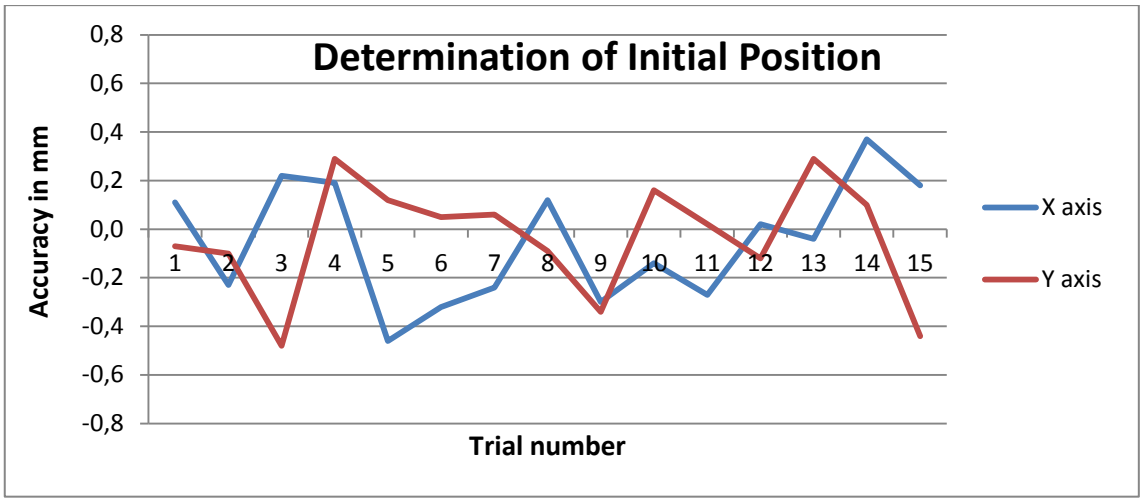

Figure 5.11. Stainless steel - Curved path – Initial position determination accuracy for X-Y directions

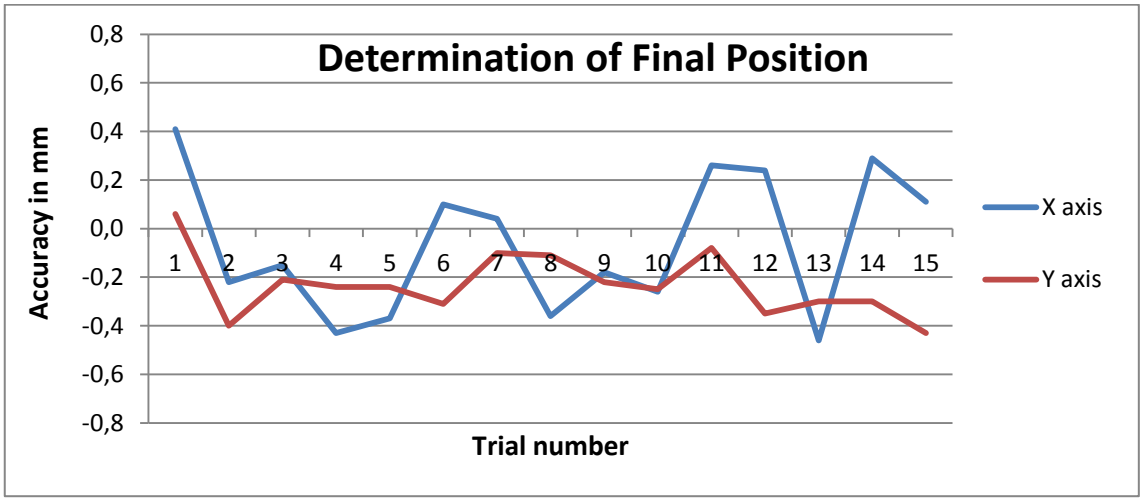

Figure 5.12. Stainless steel - Curved path – Final position determination accuracy for X-Y directions.

The distribution of allowed position determinations is presented in Figure 5.13. As it can be noticed, 52 estimates (%86,66) were within the acceptable range from 60 position determinations.

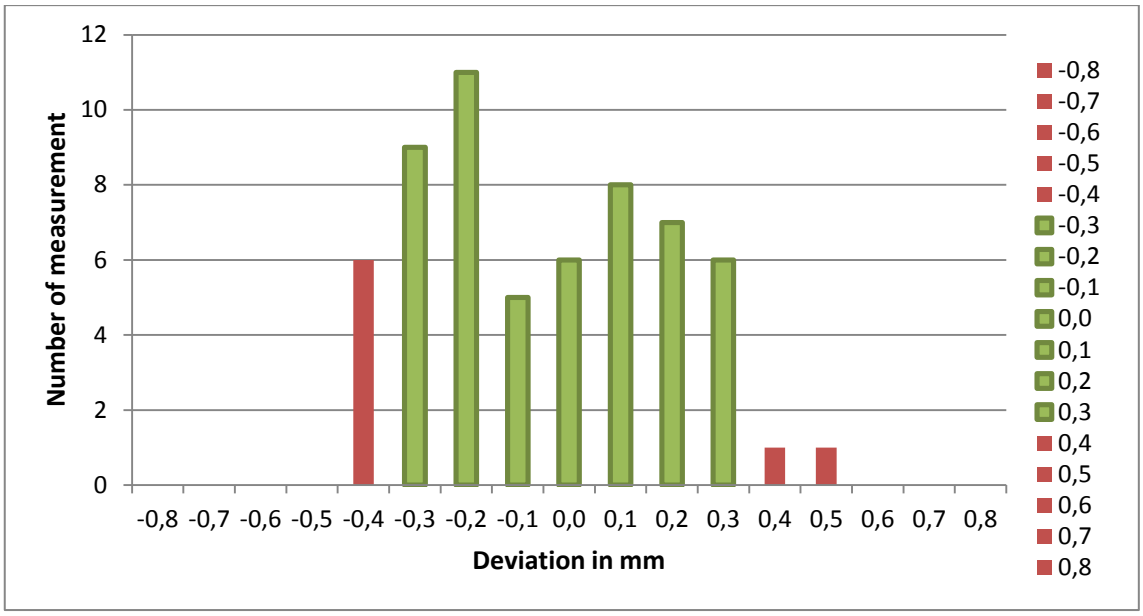

Figure 5.13. Distribution of the measurement errors for Stainless steel - Curved path experiments.

The accepted deviations are given as a performance output of vision measurement system. Varying range of errors in position determination, which are seen also in position determination figures, is as a result of surface quality of materials and the changing daylight. Therefore, surface quality of stainless steel materials has improved the initial and final point determination performance of the technique. On the other hand, vibrations on the camera resulted in blurry effect on the images that affect the determination of positions adversely.

Another experimental result during measurements is that while calibration images were being taken, unused angles and distance of checkerboard pattern affected the measurement accuracy. For instance, 16th calibration pattern of visualization, that is illustrated in Figure 5.14, is on different position when compared with other patterns which will be resulted in inaccuracies on measurements. Therefore, the 16th pattern has to be removed from calibration memory. In addition, focal distance changes during welding process influence the camera's extrinsic parameters that can result in uncertain measurements that correction of projective distortion process cannot be completed successfully.

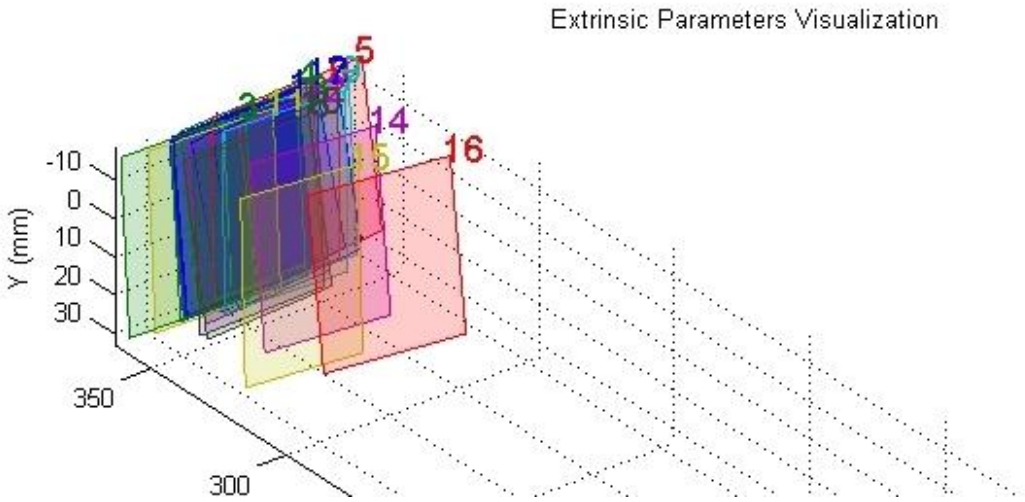

Figure 5.14 Unused position of calibration pattern.

With respect to the discussed laser welding requirements for thinner materials in Chapter 2, together with increased mating accuracy necessity, 0,3 millimeter deviation was required to be adjusted as 0,2 millimeters for successful welding (400 micron effective laser spot diameter). Therefore, performance results for less than 1mm thickness materials are:

- % 66,66 success for line path-mild steel plates,
- %70 for line path-stainless steel plates,
- %58,33 for curve path-mild steel plates and
- %61,66 for curve path-stainless steel plates.

To summarize, for thinner materials (less than 1mm thickness), higher accuracy is required for vision-based measurements.

For statistical approach, the accuracy values were estimated considering all the test results. Means are reported with %95 confidence intervals and repeatability range is given in Table 5.1.

Table 5.1. Statistical approach to measurements.

Experiment	Sample Size	Mean Error on deviations, mm	%95 confidence interval, mm	Repeatability range, mm
Line path-mild steel	60	0,2195	0,1856-0,2533	0,1339
Line path-stainless steel	60	0,2056	0,1763-0,2350	0,1159
Curve path-mild steel	60	0,2282	0,1931-0,2633	0,1386
Curve path-stainless steel	60	0,2236	0,1777-0,2695	0,1282

From the table values, it can be interpreted that the accuracy of the systems is poor since the average of deviations was found minimum 0,205 millimeters. However, repeatability, which is currently defined in ISO 9283, is the positional deviation from the average of deviations as shown in Figure 5.15. For the tests, ±0,1 millimeters repeatability indicates that any point might be as much as 0,1 millimeter beyond or short of the center of the repeatability pattern (mean error on deviations). In test results, repeatability came out to be better than accuracy since repeatability range is distributed in smaller area than overall system accuracy.

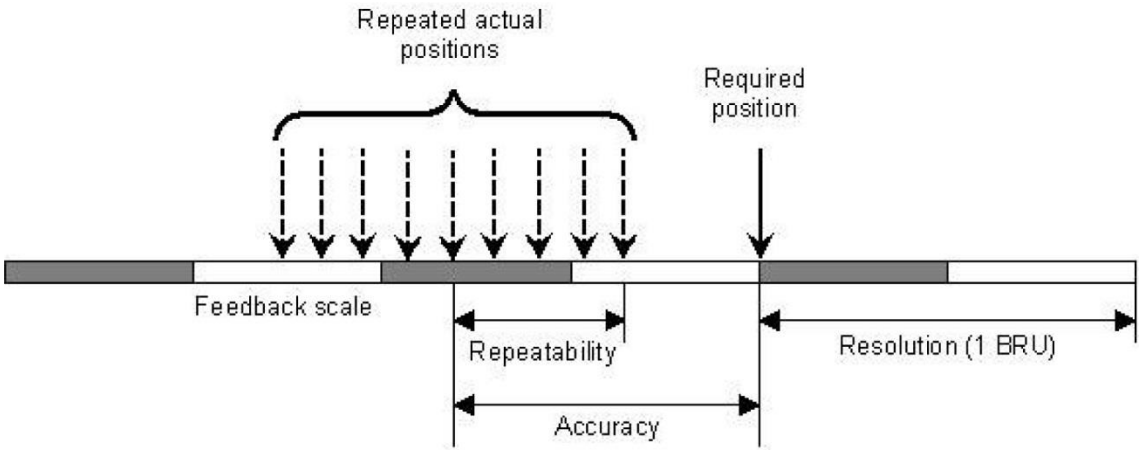

Figure 5.15. Representation of accuracy and repeatability. (ISO 9283 definition)

CHAPTER 6

CONCLUSIONS

The aim of this work is to develop welding seam identification system with the support of a vision system which is adaptable to different CNC systems. To define importance of the system for industrial environment, laser welding applications are presented in the first Chapter. Laser source units and the comparison of commonly used laser types are introduced to describe a laser beam and its advantages on welding applications. Later, the importance of laser welding automation and challenges in control process are discussed through welding parameters. The developed in-process techniques to adjust laser welding parameters during the welding operation are reviewed. Physical causes of laser welding defects are classified, which are due to high dynamics of laser welding process, lack of enough precision and existing automation challenges. Significance of pre-processing is described on laser welding when correct welding parameters are implemented for prevention of predictable defects. A review on sensing/monitoring techniques for both pre- and in-process control is represented in the literature survey. Among these techniques, the vision-based pre-processing requirements are discussed based on the insufficient accuracy and lack of information of the studies made so far. As a result of the review, the work for developing a vision-based algorithm on pre-processing task of laser welding process is summarized and later explained thoroughly.

The integration of subsystems to accommodate the developed vision-based pre-preprocessing, which comprise machine vision system and CNC system, are presented by describing the information flow through flowchart. Conversion of image position to world coordinates by a calibrated camera is demonstrated in order to present how bilateral communication of subsystems is carried out. Subroutine method is presented to adjust cycle parameters to modify main program on CNC with the export file of vision algorithm. Calculation of position and orientation correction, CNC file analysis for unmodified initial and final positions, and circle detection algorithm to detect laser spot position is developed and explained in the respective parts of this thesis.

The software and hardware parts of the experimental setup is given with the technical details of the subsystems; IPG 1kW fiber laser source unit with Precitec YW52 optical welding head, Imaging Source DFK 23U618 color industrial camera, CNC machine integrated with Power Automation industrial computer that are provided by Lazertek Tasarım Company. Software used to implement the developed technique include; DeskCNC and MATLAB Computer Vision Toolbox. Implementation of developed code by interaction of subsystems is done before initiation of full system tests.

The proposed technique provided acceptable results for both mild steel and stainless steel plates in terms of allowed deviation depending on laser spot diameter. Mean error on measurements is calculated for both line and curve path selections with respect to deviations on both X-Y directions as ± 0,22 mm. System accuracy is determined with respect to the acceptable laser beam diameter which is 600 microns. Test results revealed that the vision system accuracy changes between %85 and %95. The change of accuracy is due to changing surface contrast of materials since the performance of determining initial and final positions of welding path is affected by sharpness of acquired images, which is directly related with lighting condition. In addition, better measurement accuracy is required for thinner materials (less than 1 millimeter) due to smaller effective laser beam diameter requirements. For 400 micron diameter size, system performance is found to be decreased down to %58-70 as a result of tests.

Similar works on passive vision measurement systems to detect seam line were presented with the tracking systems by changing error deviation as ± 0,3 mm (Xu et al. 2012). Gap inspection and workpiece alignment techniques using the same vision setup was applied to butt-joint mild steel welding by using CO_2 laser with changing error deviation as ± 0,5 mm by Jeng et al. (2000).

Measurement accuracy is affected by various factors including the image processing errors due to changing light condition, material surface condition and calibration failures. Contrast failures of image under daylight results in instabilities on system measurements. One option to compensate for the lighting is to install an external light source. However, when an external light source is mounted to the system, system flexibility will be limited due to constant direction of light. Another image processing error is related with the quality of the captured image, which is affected by surface quality of welding materials. Complex surface textures can reduce the accuracy of the image processing results. From the experiments, it can be interpreted that acceptable

measurements of stainless steel materials with better surface quality can reach up to %95 measurement performance however, mild steel tests that have worse surface quality can reach up to %86 measurement performance.

Another limitation for vision systems on laser welding operations is that the vision camera cannot be mounted close to welding zone since radiated laser beam heat the environment up to 45 Celsius, which is higher than the limits of most of the vision cameras. When the vision camera is mounted at a farther distance, better focusing lens is required, which results in increased vibration for constant ROI selection and pixel errors on calibration. Therefore, the focal distances of camera and welding head have to be pre-defined properly for improved performance.

For future works, a stereo vision system to export welding path from a 3D environment. A further study can be conducted to export the welding path from a planar or 3D path independently from required CAD data in real time. For better accuracy, a co-axially mounted vision camera system that is compatible with laser welding head can be produced cost effectively. The same camera can be used for monitoring laser welding keyhole for in-process measurements. Another future work includes having a virtual working space or a vision tool with an interface to tune vision algorithm to generate position codes independently from CNC programming language.

REFERENCES

Bad'yanov, B. N. and Elizarov, A. A. 2003. "*Application of the step by step approximation method for the computer control of laser welding processes*", Measurement Techniques, Vol. 46, No. 2, pp. 5-162.

Bagger, C. and Olsen, F. O. 2003. *"Laser welding closed-loop power control"*, Journal of Laser Applications, Vol. 15, No. 1, pp. 19-24.

Banerjee, S. 2008. *"Projective geometry, camera models and calibration"*, Lecture notes of Indian Institute of Technology Delhi

Belforte, D.A. 2012, "*2011 Annual Economic Review and Forecast – A record year for industrial lasers*", Industrial Laser Solutions for Manufacturing Magazine, Pennwell Publication, USA.

Bertrand, P., Smurov, I. and Grevey, D. 2000. "*Application of near infrared pyrometry for continuous Nd:YAG laser welding of stainless steel*" Applied Surface Science 168, pp. 182-185.

Beyer, E., Behler, K., and Herziger, G. 1988. "*High-power lasers and laser machining technology*", The International Society for Optics and Photonics (SPIE), Vol. 1020, pp. 84–95.

Billion, J. P. and Fabre E. 1991. *"Industrial and scientific uses of high-power lasers"*, SPIE, Vol. 1502.

Brandner, M., Seibold, G., Chang, C., Dausinger, F., and Hügel, H. 2000. "*Soldering with solid state and diode lasers: Energy coupling, temperature rise, process window*", Journal of Laser Applications, Vol. 12, No. 5, pp. 194-199.

Brueckner, F., Hillig, H., Kempe, F., Kubisch, F., Muenster, R., Nowotny, S. & Wappler, R. 2011 *"Apparatus and method for laser deposition welding using a powdery welding material"*, U.S. Patent Application 13/088, pp. 499.

Chang, W., 2005. *"Principles of Lasers and Optics"*, Cambridge University Press, U.K.

Chang, D., Son, D., Kim, N., Kim, J., Lee, J., Kim, T. W., and Lee, K. Y. 2011. "*Development of a characteristic point detecting seam tracking algorithm for portable welding robots. In Robotic and Sensors Environments (ROSE)*", IEEE International Workshop, pp. 1-6.

Chow, W. W. and Koch, S. W. 1999. "*Semiconductor-Laser Fundamentals: Physics of the Gain Materials*", Springer-Verlag, Berlin-Germany.

Csele, M. 2004. *"Fundamentals of light sources and Lasers"*, Wiley-Interscience, USA

Dahotre, N. B. and Harimkar, S. P., 2008. Laser Fabrication and Machining of Materials, Springer Science, ABD.

DeskCNC Web site, www.deskcnc.com (accessed May 2014)

Diels, J. C., and Arissian, L. 2011. *"Lasers: The Power and Precision of Light"* John Wiley & Sons, pp. 181-201.

Dinham, M. and Fang, G. 2013. "*Autonomous weld seam identification and localisation using eye-in-hand stereo vision for robotic arc welding*", Robotics and Computer-Integrated Manufacturing, Vol. 29, No. 5, pp. 288-301.

Eddins, S. L., Gonzalez, R. C., & Woods, R. E. 2004. *"Digital image processing using Matlab"* Princeton Hall Pearson Education Inc., New Jersey.

Engström, H., and Kaplan, A. 2007. "*Adaptive Process Control in Laser Robotic Welding"*, In Proceedings of 9th NOLAMP-Conference, Trondheim, Norway..

Farson, D. 1999. "*Laser welding penetration monitoring with multiple emissions signal measurements*" Journal of Laser Applications, Vol. 11, No. 2, pp. 47-53.

Fusiello, A. 2005. *"Elements of Geometric Computer Vision"*, Homepages.inf.ed.ac.uk. accessed on 2013-12-18.

Fraunhofer institute for laser technology (ILT). 2011. "*Process control in laser material processing*".

Geiger, M., Kägeler, C., and Schmidt, M. 2008. "*High-power laser welding of contaminated steel sheets*", Production Engineering, Vol. 2, No. 3, pp. 235-240.

Gu, H. P. and Duley, W. W. 1996. "Resonant acoustic emission during laser welding of metals" J Phys. D: Appl. Phys. Vol. 29, pp.550-555.

Huang, W. and Kovacevic, R. 2011. "*A laser-based vision system for welding quality inspection*", Open Access Journal Platform, Sensors, Vol. 11, pp. 506-521

Imaging Source WEB Site, www.theimagingsource.com/ (accessed 1st of April 2014).

Injeyan, H., and Goodno, G. D. 2011. "*High power laser handbook*", McGraw-Hill Professional, USA.

Ion, J. C., 2005. *"Laser Processing of Engineering Materials"* Elsevier Butterworth-Heinemann, MA-USA.

IPG Photonics WEB Site, www.ipgphotonics.com/ (accessed 2nd of February 2014).

Jeng, J. Y., Mau, T. F. and Leu, S. M. 2000. "*Gap inspection and alignment using a vision technique for laser butt joint welding*" International Journal of Advanced Manufacturing Technology, Vol. 16, pp. 212–216.

Jingguo Ge, Zhengqiang Zhu, Defu He, Ligong Chen, 2005. "*A vision-based algorithm for seam detection in a PAW process for large-diameter stainless steel pipes.*" International Journal of Advanced Manufacturing Technology, Vol. 26, pp. 1006-1011

Jokien, T. 2004. "*Novel ways of using Nd: Yag laser for welding thick section austenitic stainless steel*", VIT Publications, Lappeeranta, Finland.

Jones, I. and Rudlin, J. 2006. *"Process monitoring methods in laser welding of plastics"* In Proceedings of The Conference Joining Plastics 2006, NPL, London

Kaierle, S. 2008. "*Process monitoring and control of laser beam welding*", Laser Technik Journal, Vol. 5, No. 3, pp. 41-43.

Kannatey-Asibu Jr, E. 2009. "*Principles of laser materials processing*". John Wiley & Sons, Vol. 4.

Kawahito, Y., and Katayama, S. 2005. *"In-process monitoring and adaptive control for stable production of sound welds in laser microspot lap welding of aluminum alloy".* Journal of Laser Applications, Vol. 17, No. 1, pp. 30-37.

Kessler, B. 2003. *"Online quality control in high power laser welding"*, White paper, Precitec KG, Germany

Kogel-Hollacher, M., Nicolay, T., Kattwinkel, A., Muller, M. G. and Muller, J. 2004. *"On-line process monitoring in laser material processing-techniques for the industrial environment",* PICALO 2004, LMP-SC, pp. 1-4.

Koechner, W. and Bass, M. 2003. "*Solid-State Lasers, Springer-Verlag*", New York, ABD.

Kong, M., Shi, F. H., Chen S. B. and Lin, T. 2007. *"Recognition of the Inıtial Position of the Weld based on the corner detection for welding robot in global environment*", Robot. Weld, Intellige. & Automation, LNCIS 362, pp. 249–255

Laserlines WEB Site, www.laserlines.co.uk/ (accessed 12th of June 2014).

Lasermech WEB Site, www.lasermech.com/ (accessed May, 2014).

Li, L., Brookfield, D. J. and Steen, W. M. 1996. *"Plasma charge sensor for in-process, non-contact monitoring of the laser welding process",* Measurement Science & Technology, Vol. 7, No. 4, pp. 615-626

Li, L. 2002. "*A comparative study of ultrasound emission characteristics in laser processing*", Applied Surface Science, Vol. 186, pp.604-610.

Matsunawa, A. 1991. "*Present and Future Trends of Laser Materials Processing in Japan*", In ECO4, International Society for Optics and Photonics. Vol. 1502, pp. 60-71.

Miyachiamerica WEB Site, www.miyachiamerica.com (accessed 14th of March 2014).

Na, X., Zhang, Y. M., Liu, Y. S. and Walcott, B. 2010. "*Nonlinear Identification of Laser Welding Process*" IEEE Transactions on Control Systems Technology, Vol. 18, pp. 927-934.

Na, X. 2010. "*Laser Welding Techniques of Real Time Sensing and Control Development*", USA.

Neto, P., and Mendes, N. 2013. "*Direct off-line robot programming via a common CAD package*", Robotics and Autonomous Systems, Vol. 61, No. 8, pp. 896-910.

Norman, P., Engström, H. and Kaplan, A. F. H. (2007, August). *"State-of-the-art of monitoring and imaging of laser welding defects"*, In 11th NOLAMP Conference in Laser Processing of Materials ,pp. 20-22.

Ono, M., Nakada, K. and Kosuge, S. 1992. "*An investigation on CO2 laser-induced plasma*", Journal of Japan Weld Society, Vol. 10, No. 2, pp. 239-245.

Ostendorf, A., Specker, W., Stallmach, M. and Zeadan, J. 2003. "*3D-MID and process monitoring for micro joining application*", High-Power Lasers and Applications, International Society for Optics and Photonics, pp. 508-517.

Ostendorf, A. and Temme, T. 2004. "*Laser spot welding of electronic micro parts*", In Fifth International Symposium on Laser Precision Microfabrication, International Society for Optics and Photonics, pp. 306-312.

Pantsar, H., Salminen, A. and Kujanpaa, V. 2001. *"Manufacturing procedure and cost analysis of laser welded all steel sandwich panels"*, In ICALEO 2001 Proceedings, Jacksonville, LIA, Orlando, pp. 1709.

Park, H and Rhee, S. 1999. "*Analysis of mechanism of plasma and spatter in CO2 laser welding of galvanized steel*", pp. 119-126.

Park, Y. W., Park, H., Rhee, S. and Kang, M. 2002. "*Real time estimation of CO2 laser weld quality for automotive industry*", Optics & Laser Technology, Vol. 34, pp. 135-142.

Petereit, J., Abels, P., Kaierle, S., Kratzsch, C. and Kreutz, E.W. 2002 *"Failure recognition and online process control in laser beam welding"*, ICALEO, 21st International Congress on Applications of Lasers and Electro-Optics, Vol. 4, pp. 9-2501.

Poppas, D. P., Choma, T. J., Rooke C. T., Klioze S. D. and Schlossberg S. M. 2005. "*Lasers in Surgery and Medicine*", Physics in Medicine and Biology, Vol. 13, No. 5, pp. 577-580.

Popov, S. 2006. "*IPG Laser GmbH fibre lasers–driving material processing markets*", In: Proceedings of AILU workshop on fibre lasers – future of laser material processing, Cranfield.

Postma, S., Aarts, R. G. K. M., Meijer, J. and Jonker, J. B. 2002. *"Penetration control in laser welding of sheet metal"*, Journal of Laser Applications, Vol. 14, No. 4, pp. 210-214.

Power Automation WEB Site, http://www.powerautomation.de/ (accessed March 2014).

Precitec WEB Site, www.precitec.de/ (accessed May, 2014)

Püskülcü, G. and Koçlular, F. 2009. "*Lazer kaynak yöntemi ve uygulamaları*", In 7th National Congress of Welding Technology, Turkey.

Quintino, L., Costa, A., Miranda, R., Yapp, D., Kumar, V., and Kong, C. J. 2007. *"Welding with high power fiber lasers–a preliminary study"*, Materials & Design, Vol. 28, No. 4, pp. 1231-1237.

Russek, U. A., Palmen, A., Staub, H., Pöhler, J., Wenzlau, C., Otto, G.and Kind, H. 2003, July. *"Laser beam welding of thermoplastics",*In High-Power Lasers and Applications, International Society for Optics and Photonics, pp. 458-472.

Sanders, P. G., Keske, J. S., Leong, K. H. and Kornecki, G. 1998. "*Real-time monitoring of laser beam welding using infrared weld emissions*", Journal of Laser Applications, Vol. 10, pp. 11-205.

Sforza, P and Blasiis, D. 2002. "*On-line optical monitoring system for arc welding*", NDT&E International, Vol. 35, pp. 37-43.

Shannon, G. J., McNaught, W., Deans, W. F., and Watson, J. 1997. "*High power laser welding in hyperbaric gas and water environments*", Journal of Laser Applications, Vol. 9, No. 3, pp. 129-136.

Shao J. and Yan Y. 2005. "*Review of techniques for on-line monitoring and inspection of laser welding*", University of Kent at Canterbuty, In Journal of Physics: Conference Series, Vol. 15, No. 1, pp. 101, IOP Publishing, UK.

Shafeek, H. I., Gadelmawla, E. S., Abdel-Shafy, A. A. and Elewa, I. W. 2004. "*Automatic inspection of gas pipeline welding defects using an expert vision system*" NDT&E International, Vol. 37, pp. 301-307.

Shen, H., Lin, T., Chen, S. and Li, L. 2010. "*Real-time seam tracking technology of welding robot with visual sensing*", Journal of Intelligent Robot Systems, Vol. 59, pp. 283-298, China.

Shi, F., Zhou, L., Lin, T. and Chen, S. 2007. *"Efficient Weld Seam Detection for Robotic Welding from a single Image",* Robot. Weld, Intelligence & Automation, LNCIS, Vol. 362, pp. 289–294.

Smith, J. S. and Lucas, J. 1989. *"A vision-based seam tracker for butt-plate TIG welding"*, University of Liverpool, UK

Steen, W. M. and Mazumder J. 2010. "*Laser Material Processing*", 4th Edition, Springer, London, UK.

Sullivan, A.B.J. and Houlcroft, P.T. 1967. "Gas-jet laser cutting" British Welding Journal, pp. 443.

Sun, A. and Kannatey-Asibu, E. 2002. "*Monitoring of laser weld penetration using sensor fusion*", Journal of Laser Applications, Vol. 14, No. 2, pp. 21-114.

Timings, R. 2008. "*Fabrication and Welding Engineering*". Elselvier, England.

Tönshoff , H. K., Ostendorf, A., Guttler, R. and Specker, W. 1998. *"Online monitoring and closed-loop control of laser welding processes*", In 12th International Symposium for Electromachining (ISEM), Vol. 11-13, No. 1405 pp. 603-612, Aachen, Germany.

Tönshoff, H. K., Körber, K., Hesse, T. and Stallmach, M. 2002. "*Increased performance and flexibility of process monitoring for deep penetration laser welding*", In ICALEO. 21st International Congress on Application of Lasers and Electro-Optics, Vol. 2, pp. 13-1105.

Trumpf-laser WEB Site, www.trumpf-laser.com (accessed 2nd of January 2014).

Unitek Miyachi Corporation 2003. "*Nd:YAG Laser welding guide*".

Warwick M and Gordon M, 2006 *"Application studies using through transmission laser welding of polymers"* In Proceedings of the conference joining plastics 2006. NPL, London.

Watson, M. N., Oakley, P. J., and Dawes, C. J. 1985. "*Metal Construction"*, pp. 25–28.

Weber, M. J. 2001. "*Handbook of lasers*", CRC Press, CA-ABD.

Wiesemann, W. 2004 *"Process monitoring and closed loop control"*, Landholt-Börnstein, Group VIII Advanced Materials and Technologies, Vol. 1C, Springer Berlin Heidelberg, XVIII, pp. 243-275.

Xu, Y., Yu, H., Zhong, J., Lin, T. and Chen, S. 2012. "*Real-time seam tracking control technology during welding robot GTAW process based on passive vision sensor*", Journal of Materials Processing Technology, Vol. 212, No. 8, pp. 1654-1662.

Zhang, X, Chen, W, Ashida, E and Matsuda, F. 2004. "*Relationship between weld quality and optical emissions in underwater Nd:YAG laser welding*" Opticas and Lasers in Engineering, Vol. 41, pp. 717-730.

Zhu, Z. Y., Lin, T., Piao, Y. J. and Chen, S. B. 2005. *"Recognition of the Initial Position of the Weld based on the image pattern match technology for welding robot*" International Journal of Advanced Manufacturing Technology, Vol. 26, pp. 784–788.

APPENDIX A

DeskCNC WITH POST-PROCESSOR

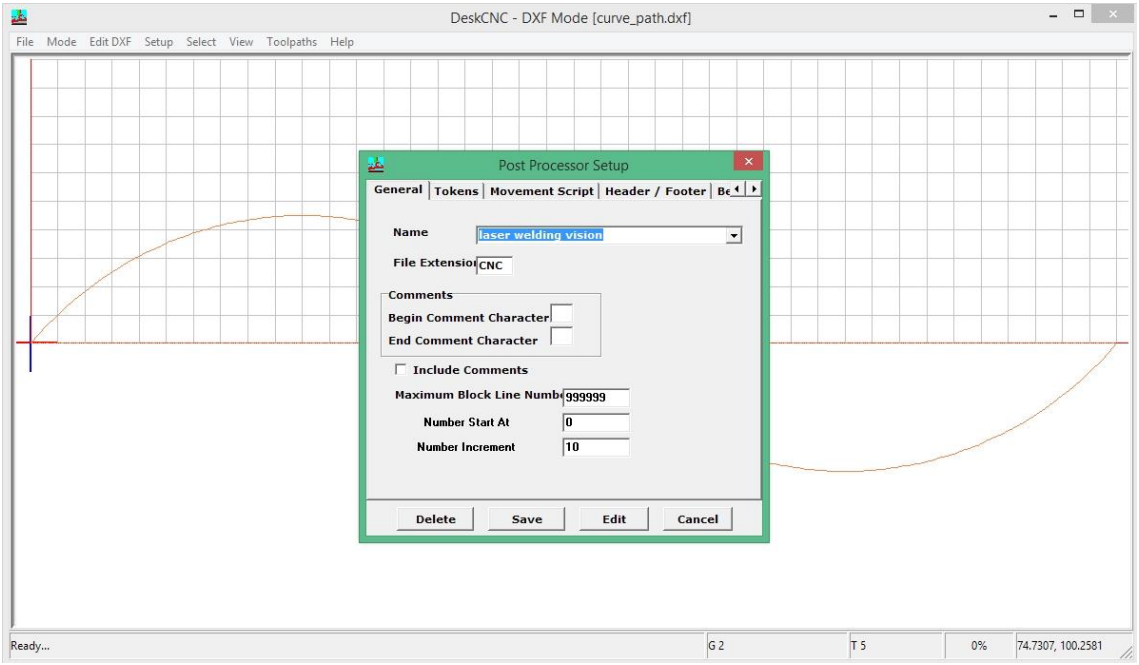

Figure A.1. Post-processor setup screen.

DeskCNC is a Windows based software that provides a CNC file preparation interface to create path and convert existing models from dxf files with a user friendly interface as illustrated in Figure A.1. Designed path by the support of CAD drawing environment (dxf files) or extracted path from an image is exported as a CNC code that contains a set of position information for use on CNC machine. For this conversion, DeskCNC provides a post-processor support which is adjustable to set required signals for various machines. To control the process of laser welding, enable signal for laser source unit and valve open signal for shielding gas has to be imported before position codes to a CNC file since they have to be activated before operation. These signals are controlled by M codes for the CNC machine signal control which is imported to header and footer tab on post-processor setup screen of software (Figure A.2). For CNC machine that is used during experimental tests, M60 is the control signal to inform the laser source unit to be ready for emission and M50 is used to open shielding gas valve

during welding operation. If there is another required signal before move and after move, it can be identified on the Before Move tab of the Post Processor Setup screen. During laser welding operation, laser emission signal is controlled with M40 and M41 codes. To open laser emission, M40 is used in the “Before Feed” section. M41 is imported “Before Rapid” section that means machine begins to move free in the operation without activating laser emission (Figure A.2).

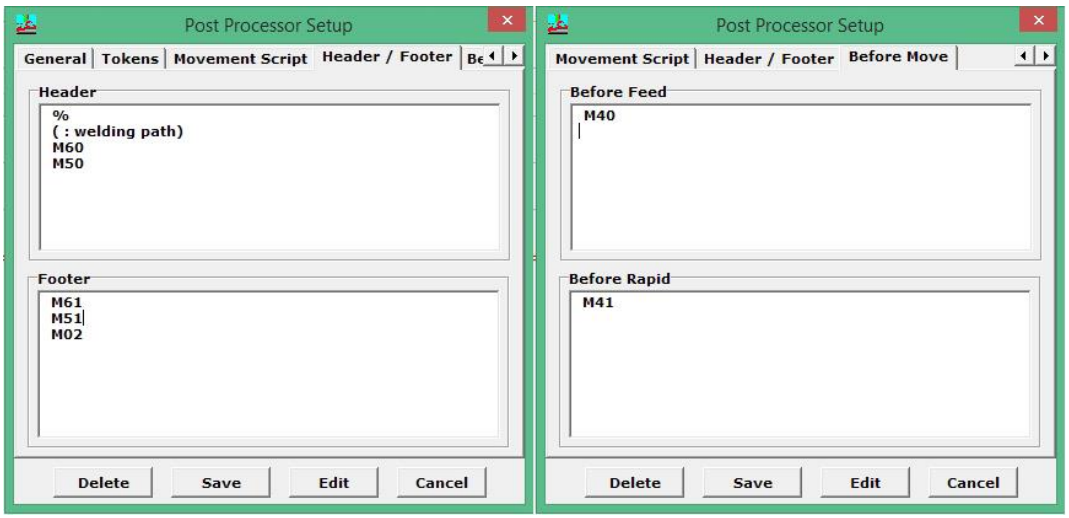

Figure A.2. Header and footer setup before position codes and laser on-off signal import screen.

After adjusted parameters are saved, imported DXF file is converted to a meaningful CNC file to be processed by the CNC machine. Exported file of a combined two curves is shown in Figure A.3 after Post Processor Setup parameters are described.

```
%
N10 ( :welding path)
N20 M60
N30 M50
N40 M40
N50 G02 X200.00 Y0.00 I100.00 J-88.61 F4000
N60 G03 X400 Y0.00 I100.00 J88.61
N70 M41
N80 M61
N90 M02
```

Figure A.3. CNC file export of two combined curves.

APPENDIX B

POWER AUTOMATION INDUSTRIAL COMPUTER

Figure B.1. Power Automation industrial computer.
(Source: Power Automation)

Power Automation industrial computer can regulate all working processes with a PC-based CNC control. Thanks to equipped high-speed microprocessor, whole transformation and compensation processes are able to run under the same computer. The technical details of computer are given in the Table B.1.

Table B.1 Technical detail of PA Industrial Computer.

Model	PA 8000 LW STD SDI-AN
CPU	Intel® Celeron™ Dual Core min. E1500 2.2GHz
USB Ports	6
Ethernet ports	1
Drive interfaces	SDI / Analogue / EtherCAT
Digital I/Os	48/32
Encoder inputs	4
Analog outputs (+/- 10V)	4
Fieldbus Extensions	PA Superbus

Power Automation Company supports user packages for variable customer demands. For laser applications, a powerful interface is provided to check signals and control welding parameters simultaneously. On the automation screen which is illustrated in Figure B.2, axis position and actual feed rate of motion are located on the top left of the screen. Laser section supports to control laser power and emission to be used in continuous or pulsed wave. “Machine” and “Head” sections are about controlling in-process cases such as cutting head height control from workpiece in case of changing surface positions of cutting plates. In machine section, necessary process parameters can be exchanged during operation practically thanks to “Parameters” function button.

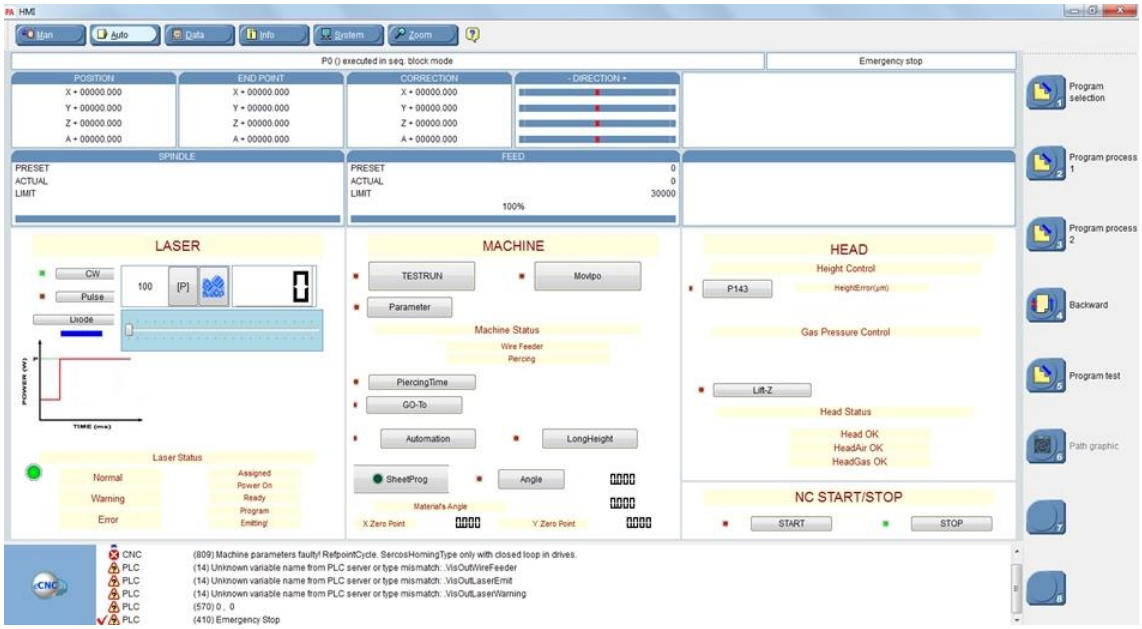

Figure B.2. Power Automation, human-machine interface to control laser power.